Postprint of: Carayon I., Szarlej P., Gnatowski P., Piłat E., Sienkiewicz M., Glinka M., Karczewski J., Kucińska-Lipka J., Polyurethane based hybrid ciprofloxacin-releasing wound dressings designed for skin engineering purpose, Advances in Medical Sciences Vol. 67 No 2 (2022), pp. 269-282. DOI: 10.1016/j.advms.2022.05.003

Polyurethane based hybrid ciprofloxacin-releasing wound dressings designed for skin engineering purpose

Iga Carayon [a,*], Paweł Szarlej [a], Przemysław Gnatowski [a,*], Edyta Piłat [a], Maciej Sienkiewicz [a], Marta Glinka [b], Jakub Karczewski [c], Justyna Kucińska-Lipka [a]

a. Department of Polymers Technology, Faculty of Chemistry, Gdansk University of Technology, Gdansk, Poland

b. Department of Analytical Chemistry, Department of Polymers Technology, Faculty of Chemistry, Gdansk University of Technology, Gdansk, Poland

c. Institute of Nanotechnology and Materials Engineering, Faculty of Applied Physics and Mathematics, Gdansk University of Technology, Gdansk, Poland

*** Corresponding author.** Department of Polymers Technology, Faculty of Chemistry, Gdansk University of Technology, Gabriela Narutowicza 11/12, 80-233 Gdansk, Poland.

E-mail address: iga.carayon@pg.edu.pl (I. Carayon); przemyslaw.gnatowski@pg.edu.pl (P. Gnatowski)

Abstract

Purpose: Even in the 21st century, chronic wounds still pose a major challenge due to inadequate potential for treatment options, so the latest wound dressings are hybrid systems that enable clinical management, such as hybrid of hydrogels, antibiotics and polymers. These wound dressings are mainly used for chronic and complex wounds, which can easily be infected by bacteria.

Materials and methods: Six Composite Porous Matrices (CPMs) based on polyurethane (PUR) in alliance with polylactide (PLAs) and poly(vinyl alcohol) (PVA) were prepared and analyzed using optical microscopy. Three different types of hydrogels and their Ciprofloxacin (Cipro) modified variants' ratios were prepared and analyzed using FTIR, SEM and EDX techniques. Six Hybrid Cipro-Releasing Hydrogel Wound Dressings (H-CRWDs) were also prepared and underwent short-term degradation, Cipro release, microbiology and cell viability measurements.

Results: Average porosity of CPMs was in the range of 69-81%. The pore size of the obtained CPMs was optimal for skin regeneration. Short-term degradation studies revealed degradability

in physiological conditions regardless of sample type. A meaningful release was also observed even in short time (21.76 ± 0.64 μg/mL after 15 min). Microbiological tests showed visible inhibition zones. Cell viability tests proved that the obtained H-CRWDs were biocompatible (over 85% of cells).

Conclusions: A promising hybrid wound dressing was labeled. Simple and cost-effective methods were used to obtain microbiologically active and biocompatible dressings. The results were of importance for the design and development of acceptable solutions in the management of chronic wounds of high potential for infection,

Keywords: polyurethane; polylactide; composite; ciprofloxacin; skin engineering

1. Introduction

Skin is one of the largest organs in the human body and compromises about 10% of body weight. It acts as a barrier, protecting against the loss of fluids, important for maintaining body homeostasis, and also makes a cover against mechanical and thermal injuries of internal organs. Furthermore, skin acts like an isolation for tissues and organs against harmful external factors (chemical substances, biological pathogens and UV radiation) [1]. Due to its functions, skin is exposed to various types of damage leading to formation of different kinds of wound, like: burn wounds, diabetic ulcers, venous leg ulcers, chronic wounds, etc. [2].

Human skin has great potential to regenerate after injury through the hierarchically arranged physiological processes such as: coagulation and hemostasis, inflammation, proliferation and remodeling [3,4]. Usually these steps allow for total regeneration of normal wounds [5]. Unfortunately, it is not the case for chronic wounds, which are often defined as wounds that do not regenerate in 90 days [6]. Their healing process is a great therapeutic challenge [7]. Chronic wounds can be caused by many factors, including infection with bacteria or antibiotic-resistant pathogens. Traditional forms of dressings often are dry and do not provide proper wound regeneration environment which can lead to adhesion to the wound leading to difficult and painful removal process [8]. Moreover, traditional dressings have to be replaced often because of the limited possibilities of exudates absorption [9]. Luckily, chronic wounds healing process can be supported by many types of wound dressings and tissue scaffolds, which can be classified as drug delivery systems (DDSs). The main task of DDSs is to deliver the suitable dose of active substance at the right time to a specific place, without causing side effects [6,10]. In addition, controlled release systems allow modification of the drugs dose and provide stability of active substance in physiological conditions [11].

Nowadays, the therapy of the various types of wounds uses novel, specially designed dressings based, in example, on hydrogels [12], polyurethane fibers [13] or foams [14], alginates [15], collagens [16], hydrofibers [17] and hydrocolloids [18,19]. The choice of the proper type of dressing depends mainly on the type of wound, the healing phase of dressing application and also dressing desired function (absorption of exudation, hydration of wound, occlusive function or antibacterial effect) [20–23]. Materials most commonly applied as a wounds treatment exhibit healing properties according to the TIME concept (Tissue, Infection, Moisture, Edge), which means that they provide a moist healing environment, protection of wound edges, resistance to contaminations, allow gas exchange and control of infection [23,24]

Recent trends in wound dressings design is focused on application of synthetic polymer compositions containing polyurethanes (PURs). PURs are considered as one of the most biocompatible and hemocompatible synthetic polymers available on the market these days [25]. PURs are commonly used biomaterials in medical applications and devices (catheters, aortic balloons, implants, etc.). Their broad application spectrum is related to their unique structure and properties like significant flexibility, good biocompatibility in vitro, non-toxic degradation products [26]. Moreover, through different modifications, PURs biological activity and attractiveness for cells proliferation can be adjusted [27]. Among other synthetic polymers polylactide (PLAs) and poly(vinyl alcohol) (PVA) are also great candidates for usage in the skin engineering field. Both PLA and PVA represents good biocompatibility and biodegradability – features needed in the field of tissue engineering of skin.

To provide suitable antibacterial protection, fluoroquinolones are applied as a factor that enhances the regeneration of infected wounds. Fluoroquinolones show wide antibacterial activity and they are effective against *Eschericha coli* (*E. coli*) and *Staphylococus aureus* (*S. aureus*), which are the most common bacteria responsible for wound infections [28,29]. For example, Sripriya et al. [30] produced collagen bilayered dressings with ciprofloxacin (Cipro) for infected wounds. *In vitro* assays proved their effectiveness against *S. aureus* and *P. aeruginosa.* Furthermore, *in vivo* tests on rats showed increased regeneration process in the group treated with collagen bilayered dressing containing Cipro. It was observed that sustained release of Cipro from obtained dressings eliminates the bacteria occurring in wounds. Additionally, Choipang et al. [31] in 2018 obtained PVA hydrogel dressings containing poly(D,L-lactide-*co*-glycolide) (PLGA) and Cipro hydrochloride nanoparticles. Their effectiveness was confirmed against *E. coli* and *S. aureus*.

In our team, we had been working on synthesis and fabrication of antibacterial scaffold obtained with the use of PUR/PLA blends and modified with Cipro. Kucińska-Lipka et al. has described design, synthesis and characterization of PURs crosslinked with PVA as a new proposition for regenerative medicine. Performed characterization showed that tensile strength of the materials was in the range of 41–52 MPa and contact angle of their surface was in the range of 38–47°. The obtained PVA-crosslinked PURs did not show significant progress of degradation after 3 months of incubation in a phosphate-buffered saline (PBS). Thus, obtained materials may act as a slowly-degradable material, which can provide long-term physical support in tissue engineering purpose. A performed short-term hemocompatibility study showed that obtained PVA-crosslinked PURs do not significantly influence blood components and a cytotoxicity test, performed with the use of MG 63 cell line, revealed the great cytocompatibility of the obtained

materials [32]. Carayon et al. fabricated antibacterial and degradable scaffolds that may be used in the field of skin regeneration. Degradable PURs were obtained by using amorphous α,ω-dihydroxy(ethylene-butylene adipate) macrodiol (PEBA). PURs were processed with PLA (5 or 10 wt%). To meet the antibacterial requirement, the previously obtained hybrid PUR-PLA scaffolds (HPPS) were modified with Cipro (2 or 5 wt%). Performed studies showed that Cipro-modified HPPS, obtained by using 5 wt% of PLA, possess suitable mechanical characteristics, morphology, degradation rates, and demanded antimicrobial properties to be further developed as potential scaffolds for skin tissue engineering [33].

To meet the requirements of skin engineered substitutes we proposed a fabrication of hybrid ciprofloxacin-releasing wound dressing (H-CRWD). H-CRWD is a combination of solid composite porous matrix (CPM) covered with Cipro-loaded biocompatible hydrogels (CLHs). CPMs were obtained with the use solvent casting/particulate leaching technique (SC/PL) and consist of composition of PUR/PLA or PUR/PVA at different concentrations (10, 20 or 30 wt%). CPM is coated with hydrogel, which is loaded with Cipro (CLHs) to provide immediate antibacterial action after wound dressing application on the burned, wounded or traumatized skin. Produced H-CRWDs represents suitable physicochemical properties, favorable morphology, degradation rate, and satisfactory biological performance when CPMs are composed of PUR/30PVA. Such hybrid wound dressings, currently fabricated in a laboratory scale, may be the future simple and cost-effective solutions to treat chronic and complex wounds, which are one of the biggest medical challenge of 21st century.

2. Materials and methods

2.1. Materials fabrication

2.1.1. Composite Porous Matrices (CPMs) Fabrication

CPMs were fabricated by simple and cost effective solvent casting/particulate leaching (SC/PL) technique. In the first step 100g of polymer mix containing PUR (Epaline Epaflex 380 A 10 25), PLA (Ingeo 7032D) or PVA (Mowiol 4-88 Mw 31,000) (10, 20 or 30% w/w) was prepared. Then PUR/PVA mixes were dissolved in DMSO and the PUR/PLA mixes were dissolved in THF/DMSO mixture (1:6 w/w). Solutions were stirred at reflux at 90°C until dissolution of polymers. Weight concentration of PUR/PLA and PUR/PVA polymer mixtures in DMSO and THF/DMSO solutions were equal to 20%. In the next step sodium chloride (diameter fraction of 50 – 200 μm) was added as a porogen to 10 grams of obtained homogeneous solutions under rigorous mixing. Sodium chloride was being added to the mixture until a paste-like consistency

was obtained (40 g of NaCl). The mixture was then transferred to glass, round molds (10 cm diameter and 0.5 cm height) and placed in freezer for 48h at -20 °C. The obtained thin matrices were submerged in distilled water for 7 days, and then dried for 1 day at 60°C. Symbols and description of obtained matrices were listed in the **Table 1**.

Table 1. Symbols of obtained Composite Porous Matrices (CPMs) with their brief description.

Symbol	Description
PUR/10PLA	Matrices made of PUR and 10 wt% of PLA
PUR/10PVA	Matrices made of PUR and 10 wt% of PVA
PUR/20PLA	Matrices made of PUR and 20 wt% of PLA
PUR/20PVA	Matrices made of PUR and 20 wt% of PVA
PUR/30PLA	Matrices made of PUR and 30 wt% of PLA
PUR/30PVA	Matrices made of PUR and 30 wt% of PVA

2.1.2. Cipro-Loaded Hydrogels (CLHs) Fabrication

Unmodified hydrogels were obtained as follows: solution of PVA (4 wt%) and Borax (2 wt%) were prepared in distilled water (70°C/16h, magnetic stirring). Solution of PVA and Borax were mixed together to obtain 100 grams of solution at 1:3, 1:2 and 1:1 ratio at 90°C and stirred for 2h. After that time homogenous solutions were obtained.

To load ciprofloxacin hydrochloride (Cipro) within hydrogel's net, following steps were undertaken: Cipro (1.5 wt%), L-ascorbic acid (10 wt%, LAA) and PVA (4 wt%) were mixed together at 90°C for 2h. After that time, Borax solution (2 wt%) was added to the homogenous solution of PVA containing Cipro and LAA at three different ratios: 3:1, 2:1 or 1:1 to obtain 100 grams of solution. LAA was used to reduce pH to acidic values and prevent precipitation of Cipro. Due to this step, obtained PVA-Cipro-LAA solutions were homogenous while mixing with Borax solution. Symbols and descriptions of both unmodified (Table 2. H1-H3) and Cipro-modified hydrogels (Table 2. H4-H6) were listed in **Table 2**. Solutions at all ratios were transferred into round molds and dried for 24h at 20°C.

Table 2. Symbols of obtained CRHs with their brief description.

	Symbol	Description
Unmodified hydrogels	H1	Hydrogel made of PVA and borax solutions in ratio 1:1 (w/w)
	H2	Hydrogel made of PVA and borax solutions in ratio 2:1 (w/w)

	H3	Hydrogel made of PVA and borax solutions in ratio 3:1 (w/w)
Modified hydrogels	H4	Hydrogel made of 4% PVA, 1.5% Cipro and 10% AA solution and mixed with a borax solution in ratio 1:1 (w/w)
	H5	Hydrogel made of 4% PVA, 1.5% Cipro and 10% AA solution and mixed with a borax solution in ratio 2:1 (w/w)
	H6	Hydrogel made of 4% PVA, 1.5% Cipro and 10% AA solution and mixed with a borax solution in ratio 3:1 (w/w)

171

172 2.1.3. Hybrid Cipro-Releasing Hydrogel Wound Dressing (H-CRWD) Fabrication

173 An immersion technique was used to fabricate H-CRWDs. Obtained CPMs (Table 1) were
174 immersed in hydrogels solutions (Table 2) for 1h at 90°C (to prevent premature gelation
175 process). After that, obtained H-CRWDs were transferred to the drier and dried for 24h at 40°C.
176 **Table 3** summarizes content of all H-CRWDs. **Fig. 1** visualizes the step-by-step process of H-
177 CRWDs fabrication.

178

179 **Table 3.** Symbols of obtained Cipro-Releasing Hydrogel Wound Dressings (CRWDs) with
180 their brief description.

181

Symbol	Description
D1	Dressing made of PUR/30PLA matrix covered with H4
D2	Dressing made of PUR/30PLA matrix covered with H5
D3	Dressing made of PUR/30PLA matrix covered with H6
D4	Dressing made of PUR/30PVA matrix covered with H4
D5	Dressing made of PUR/30PVA matrix covered with H5
D6	Dressing made of PUR/30PVA matrix covered with H6

182

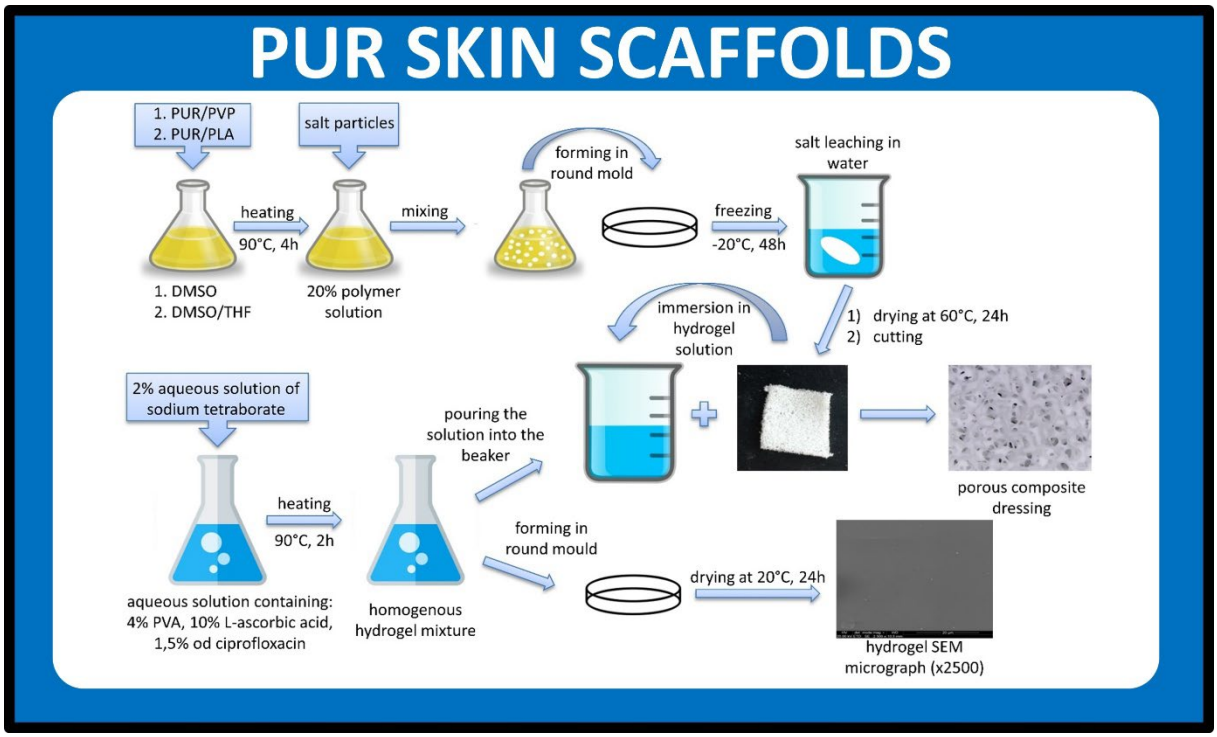

Figure 1. Scheme of hybrid composite porous matrices development.

2.2. Characterization techniques

2.2.1. Fourier transform-infrared spectroscopy (FTIR)

Examination of samples using the FTIR spectrometer allows the determination of characteristic vibrations for functional groups occurring in the material. To demonstrate the presence of characteristic bonds in the obtained hydrogels, samples were tested with a Nicolet 8700 spectrometer (Thermo Electron Corporation, Wilmington, DE, USA) equipped with a Specac's Golden Gate and a single reflection diamond ATR unit. The study was conducted at a resolution of 4 cm^{-1}. Each sample was tested using 256 scans per sample in the spectral range from 4000 to 500 cm^{-1}.

2.2.2. Scanning electron microscopy (SEM) with Energy-dispersive X-ray spectroscopy (EDX)

The hydrogels morphology was examined using an FEI QUANTA 250 FEG SEM microscope (Thermo Fisher Scientific, Waltham, MA, USA) at an accelerating voltage of 20 kV and magnification of 1000x and 2500x. To determine the atomic composition of the produced hydrogel dressings, an energy-dispersive X-ray spectrometer was used. The scanning time of measurement was 200 s per sample. Before analysis hydrogels were cut into cylindrical samples (diameter = 0.8 cm, area = 0.5 cm^2) and covered with gold using a sputter Quorum 150T E

(Quorum Technologies, Laughton, East Sussex, UK). EDX analysis was performed 3 times for each sample type.

2.2.3. Optical microscopy, pore sizes and porosity

Morphology assessment of obtained porous matrices before and after degradation was done using the Digital Microscope, model avp028f8 certified by FC & CE (Flood Control and Coastal Emergency) and RoHS (Restriction of Hazardous Substances). The images were observed using magnifications of 40x and 800x. To record microscopic images, a desktop computer with VidCap software was used. Obtained images allowed also to determine the size and type of pores and additionally evaluated the interconnection of pores. ImageJ Software (Rasband, W.S., ImageJ, U. S. National Institutes of Health, Bethesda, Maryland, USA, https://imagej.nih.gov/ij/, 1997-2021) was used to analyze microscopic images. The porosity was measured using the following equation (1):

$$P = 1 - \left(\frac{V_1 - V_2}{V_2 - V_3}\right) x\ 100\ \% \quad (1)$$

Where:

V_1 - volume of ethanol [cm^3];

V_2 - volume of ethanol after immersion of matrix [cm^3];

V_3 - volume of ethanol after removal of matrix [cm^3].

2.2.4. Short-time degradation (STD) study

Studies of the degradation were carried out in 5M NaOH, 2M HCl and 0.01 PBS (Phosphate-buffered saline) aqueous solutions. Round samples (diameter = 0.7 cm, area = 0.38 cm^2, thickness = 0.2 cm) were cut out from obtained porous matrices. Three samples were taken from each type of matrix and were stored in the 1.5 ml solution of selected medium. The degradation process was performed at 37 °C for 7 and 14 days (5M NaOH and 2M HCl) or for 1, 7, 14, 28 and 56 days (0.01M PBS). Before the studies, samples were dried and weighted using Thermobalance (RADWAG MAX50/SX) set at 60 °C. After the degradation process the samples were rinsed with distilled water, dried at 60 °C for 24 h and weighted again. The mass loss of the samples was measured by following formula (2).

$$M = \left(\frac{m_i - m_0}{m_0}\right) \times 100\ \% \quad (2)$$

Where:

M - mass loss [%];

m_0 - initial mass [g];

m_i - mass after degradation process [g].

2.2.5. High Performance Liquid Chromatography (HPLC)

The release of active substances from produced composite dressings (D1-D6) was performed using a Agilent 1200 LC system consisting of ALS autosampler, binary pump, degasser, thermostated column compartment and DAD detector (λ = 277 nm). The chromatographic separation an active substance (Cipro) was carried out using ZORBAX Eclipse XDB-C8 (Agilent) LC column (150 x 4.6 mm, 5 µm) using isocratic conditions with mixture of 0.02 M KH_2PO_4 solution (acidified to pH = 2.7) and acetonitrile (80:20 v/v). Flow rate of 0.8 mL/min was used and injection volume was established as 20 µl. Temperature of column was maintained at 35 °C. Cipro calibration was realized using external calibration method. Working standard solutions (0.5, 1, 5, 10, 50, 100 µg/mL) were prepared daily by dilution of stock solution with distilled water and analyzed in triplicate (n = 3). Real-world samples (D1-D6) were cut into pieces with diameter = 0.7 cm, and thickness = 0.2 cm). In following step, prepared samples were immersed in deionized water (5 mL) and incubated at 37°C. After specified time of incubation, for each sample the water phase was analyzed. Samples were prepared and analyzed in triplicate.

2.3. Statistical analysis

The statistical analysis was performed with the use of the Origin Pro 8.5 software (OriginLab Corporation, Northampton, MA, USA). To determine the statistical differences, one-way ANOVA (α = 0,05), two-way ANOVA (α = 0,05) and post-hoc Tukey test (α = 0,05) (n=3) were used.

2.4. Biological Performance

2.4.1. Microbiology tests

Microbiological tests were performed with a use of H-CRWDs based on PUR/30PLA and PUR/30PVA systems modified with hydrogels (H4-H6, Table 2) containing 1.5% of Cipro. Selection of H-CRWDs containing 30 wt% of PLA or PVA in a PUR/PLA or PUR/PVA composition was dictated by their porosity, which was the highest for those compositions. For comparison, hybrid wound dressings based on PUR/PLA or PUR/PVA were fabricated in exactly same way as it was in case of H-CRWDs, with a step exclusion related to their modification with Cipro. Neat hybrid wound dressings served as a control.

Methodology of microbiological tests was similar to the one previously published [33]. *Staphylococcus aureus* (Gram positive). Selected bacterial strain was cultivated in 20 ml of fresh and sterile Luria broth (LB) medium. The LB medium contained: casein peptone 10.0 g/L; yeast extract 5.0 g/L; NaCl 10.0 g/L dissolved in deionized water. Cultivations were carried out in 200 ml sterile Erlenmeyer flasks on a rotary shaker at 170 rpm at 37 °C for 18–24 h. After the incubation time, 100 µL of each bacterial strain culture was transferred into 10 mL of sterile LB medium in 100 mL sterile Erlenmeyer flasks. Next, bacterial strains cultivations were carried out on a rotary shaker at 170 rpm at 37 °C to get the log phase of bacterial growth (OD600 values 0.4–0.7). For determination of antibacterial activities, 100 µL of each bacterial strain suspensions in the log phase of growth were placed on sterile LA medium with a sterile glass rod. The LA medium contained: casein peptone 10.0 g/L; yeast extract 5.0 g/L; NaCl 10.0 g/L; agar 15.0 g/L dissolved in deionized water. Prior to the examination, unmodified and Cipro-modified HPPS were sterilized by the exposition to UV radiation for 30 min and placed on plates with sterile tweezers. Sterile samples of unmodified and Cipro-modified HPPS scaffolds were placed on bacterial cultures on LA plates and incubated at 37 °C for 24 h. After the incubation, the diameter of the presence or absence of growth inhibition zones around samples of unmodified and Cipro-modified HPPS was measured. All analyses were done in triplicate.

2.4.2. Cytotoxicity Assay

Cytotoxicity of obtained H-CRWD obtained with the use of PUR/30PVA was studied according to the ISO 10993-5 standard in indirect cytotoxicity test using MTT assay. This selection was dictated by the favorable properties of these samples reached in short-term degradation test and drug release study.

Samples were sterilized 30 min each side under UV radiation. Then, an extract of studied samples was prepared in culturing medium DMEM/F-12 supplemented with FBS; 5 µg/ml penicillin with streptomycin; 5 µg/ml amphotericin B (Corning). Prepared extracts were incubated for 24 h at 37 °C and 5% CO_2. After that time, extracts were filtrated and placed in the culturing wells with CCl163 cells, which were cultured as follows: cells were seeded on 24-well culture plates with a density of 19 000 cells per 1 cm^2 (ThermoFisher) and cultured for 24 h at 37 °C and 5% CO_2 in the supplemented DMEM/F-12 culturing medium (Corning). After 24 h of cells incubation with extract, the MTT assay was performed. The absorbance of prepared solutions was studied by using Spectrophotometer set at $\lambda = 570$ nm (ThermoFisher). The results were were showed in the graph as cells viability towards control (100% of viability).

The statistical analysis was performed with the use of the Origin Pro 8.5. Statistical differences were evaluated by the one-way ANOVA ($\alpha = 0.05$) and post hock Tukey test ($\alpha = 0.05$).

3. Results

3.1. Composite Porous Matrices (CPMs) Characterization

3.1.1. Optical microscopy and porosity calculation

Microscopic images of CPMs were shown in **Fig. 2**. Obtained CPMs were characterized by average porosity ranging from 69 to 81 %. Detailly, for PUR/10PLA, PUR/20PLA and PUR/30PLA CPMs porosity was determined as follows: 69.22 ± 2,01%, 73.06 ± 2.33% and 72.03 ± 2.04%, respectively (**Figure 3**). One-way ANOVA test confirmed that those values were not statistically different ($\alpha = 0.05$).

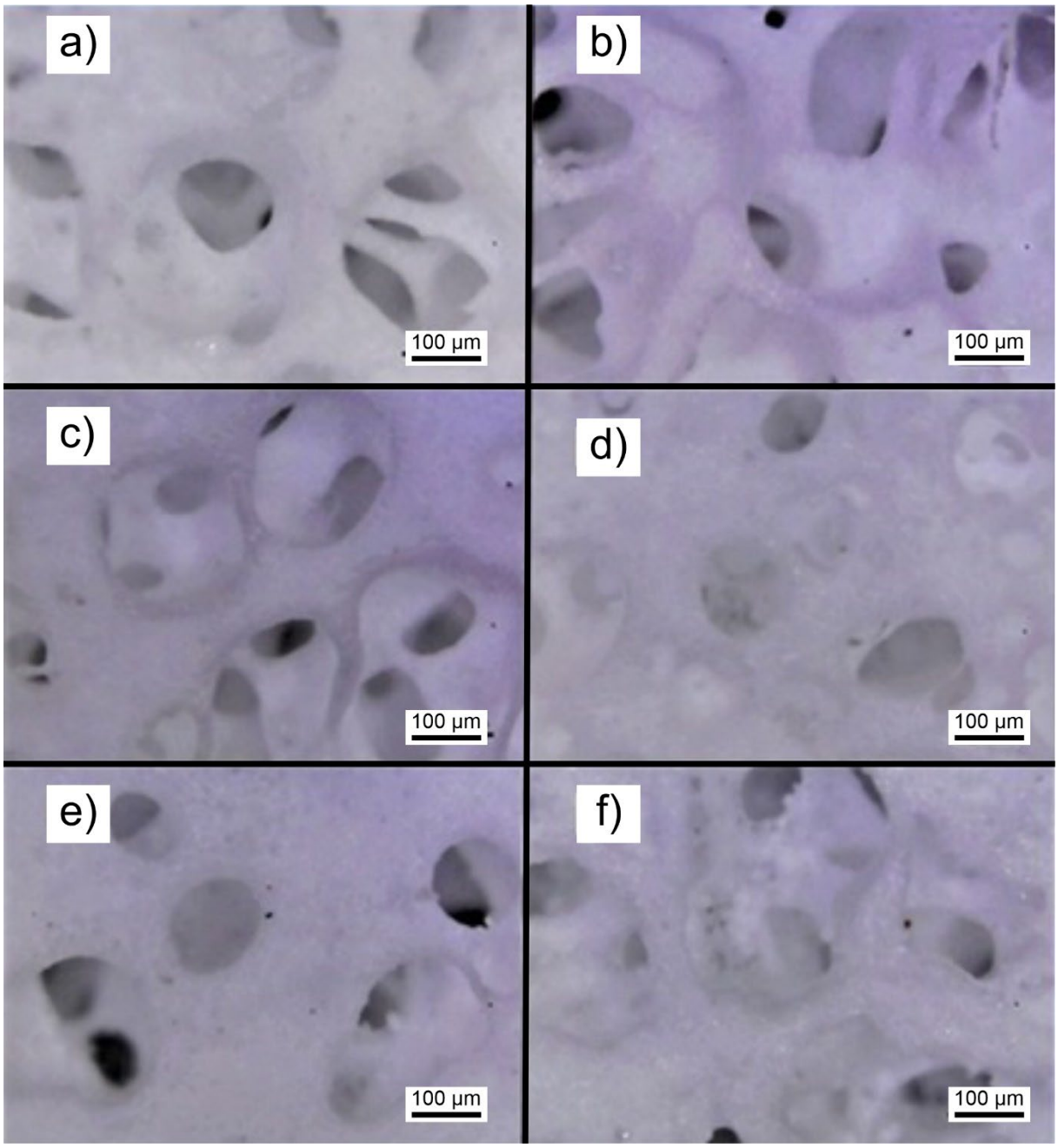

Figure 2. Optical microscopy of CPMs: a) PUR/10PVA, b) PUR/20PVA, c) PUR/30PVA, d) PUR/10PLA, e) PUR/20PLA, f) PUR/30PLA. Magnification of 800x.

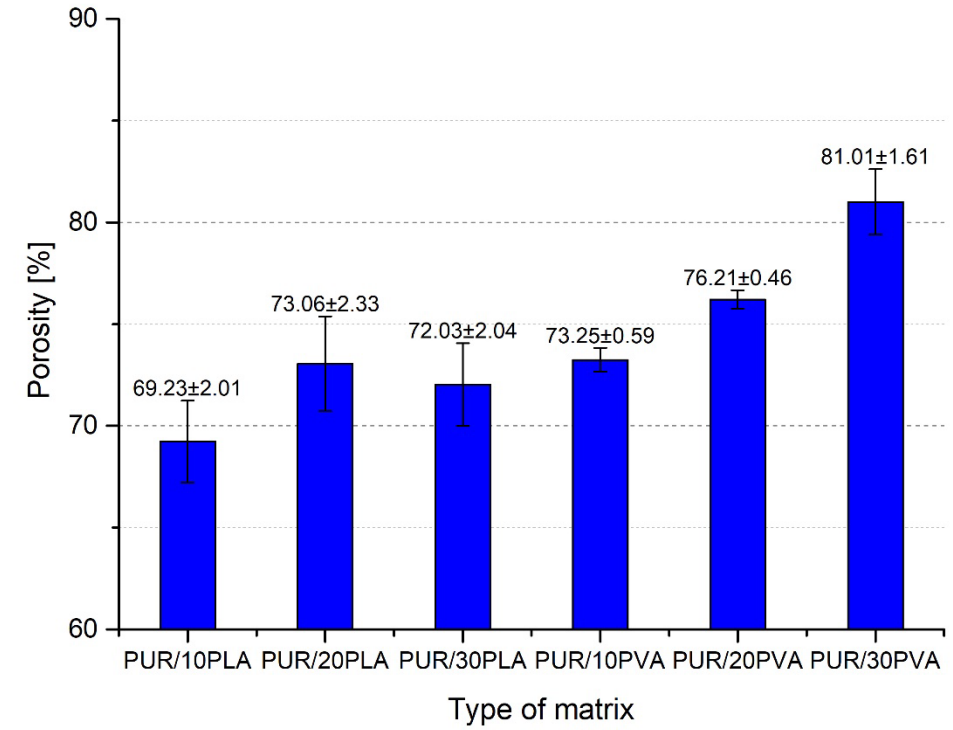

311

312 **Figure 3.** Average porosity of obtained CPMs.

313

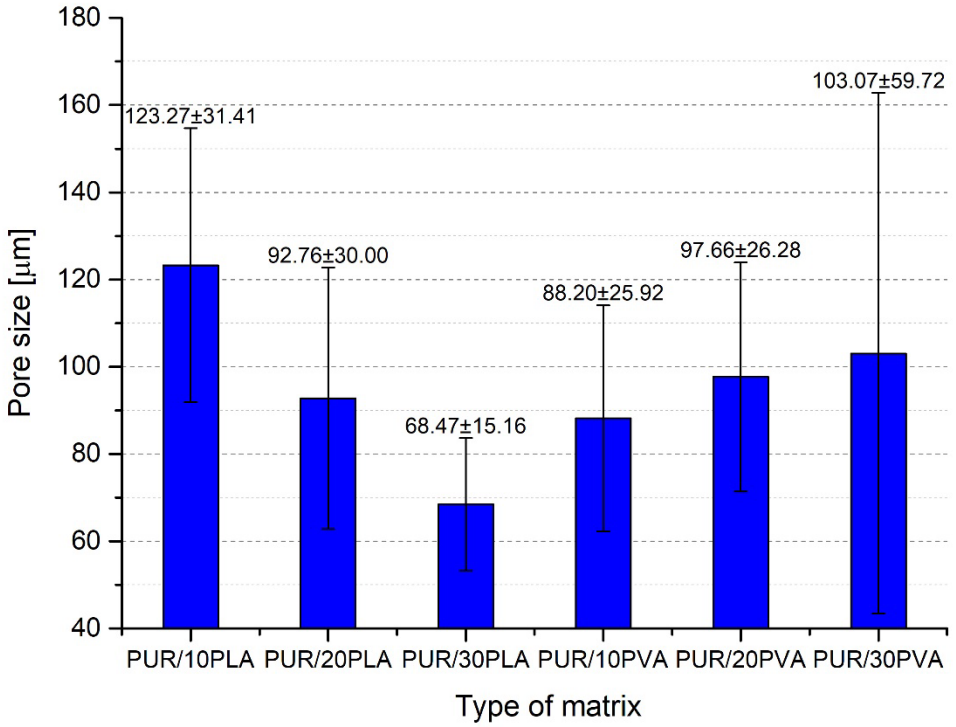

314

Figure 4. Average pore sizes of obtained CPMs.

However, for PUR/10PVA, PUR/20PVA and PUR/30PVA samples identified porosity was slightly higher (73.25 ± 0.59%, 76.21 ± 0.46% and 81.01 ± 1.61%, respectively, **Figure 3**) in comparison to CPM obtained with the use of PUR/PLA composition. One-way ANOVA statistical evaluation determined, that mean porosity values for PUR/10PVA and PUR/20PVA were not statistically different ($\alpha = 0.05$). However, Tukey test evaluated that porosity for PUR/30PVA was significantly higher than for PUR/10PVA and PUR/20PVA ($\alpha = 0.05$). It can be considered that the type of added component in a composite, in this case PLA or PVA, affects porosity of obtained composites.

PUR/PVA samples were characterized by a porosity higher by 5% on average in comparison to PUR/PLA samples. Despite this identified difference both CPM (PUR/PLA and PUR/PVA) were described as suitable for the purpose of skin engineering.

Computer analysis of CPMs images (**Figure 2**) revealed that PUR/10PLA matrix was characterized by high average pore sizes equal to 123.27 ± 31.41 μm (**Figure 4**). This value was slightly higher than average pore size calculated for PUR/20PLA and PUR/30PLA matrices, which reached 92.76 ± 29.99 μm and 68.47 ± 15.16 μm, respectively ($\alpha = 0.05$).

For PUR/10PVA, PUR/20PVA and PUR/30PVA samples average pore sizes were similar with the amount of PVA in a composition: 88.20 ± 25.92 μm, 97.66 ± 26.28 μm and 103.07 ± 59.72 μm, respectively. One-way ANOVA test proved that pore size values for PUR/PVA composite matrices were not statistically different ($\alpha = 0.05$). It was also found that the addition of PLA causes a decrease in porosity with its increasing amount, while the growing addition of PVA increases the average pore size diameter.

3.2. Unmodified hydrogels (UnMHs) and Cipro-Loaded Hydrogels (CLHs) Characterization

3.2.1. Fourier transform infrared spectroscopy (FTIR)

FTIR spectra of native PVA, and UnMHs (**Table 2**, H1-H3) were presented in **Fig. 5**. Detailed band assignments were given in **Table 4**.

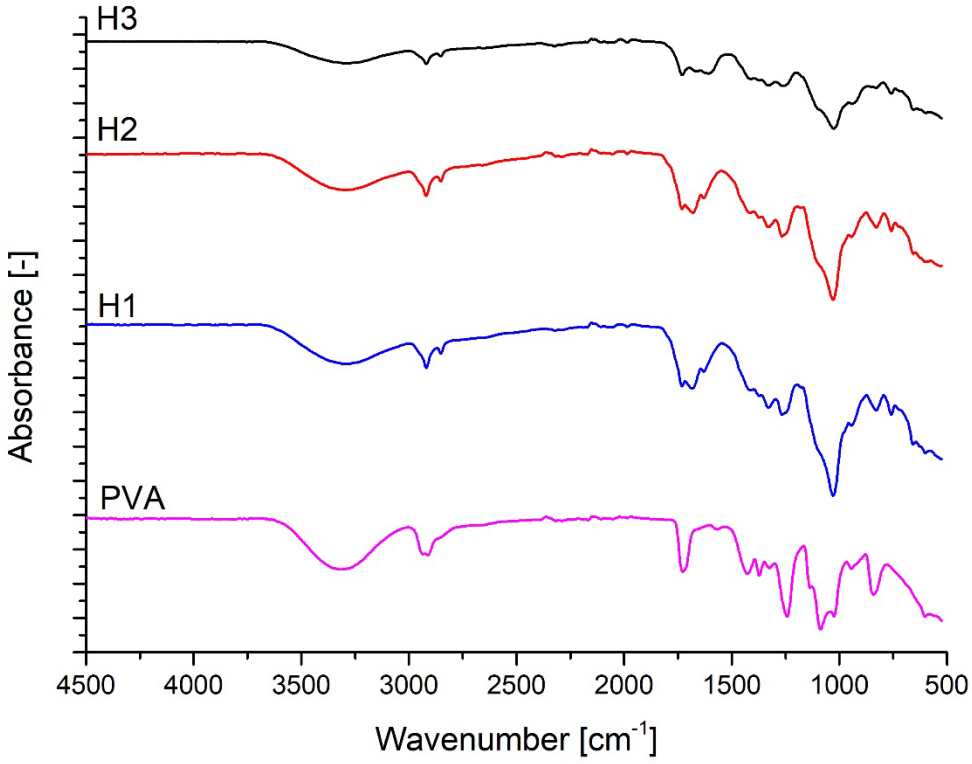

343

344 **Figure 5.** FTIR spectra for native PVA and UnMHs.

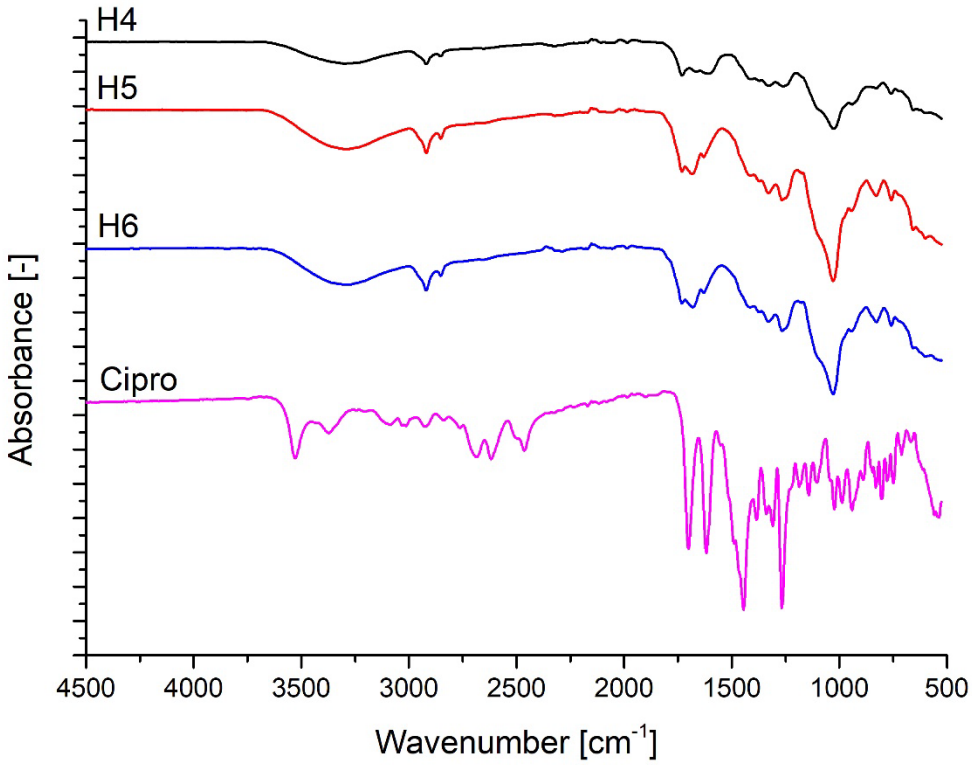

345

346 **Figure 6.** FTIR spectra for CLHs and Cipro.

Table 4. Detailed band assignment of Fourier transform-infrared spectroscopy (FTIR) spectra presented in Fig. 5 (PVA and UnMHs).

Wavelength [cm^{-1}]	Assignment
3600-3100	ν(O-H) stretching vibrations from hydroxyl groups of PVA and H1, H2, H3 hydrogels
2930	ν(C-H) symmetrical stretching vibrations from CH_2 groups
2850	ν(C-H) asymmetrical stretching vibrations from CH_2 groups
1740	ν(C=O) stretching vibrations from acetyl groups
1500-1300	δ(C-H) deformation vibrations from CH_2 groups
1290	ν(B-O-C) stretching vibrations from H1, H2 and H3 hydrogels
1250	ν(C-O) stretching vibrations from acetyl groups
1130	ν(B-O-C) stretching vibrations from H1, H2 and H3 hydrogels
1100	ν(C-O) stretching vibrations from C-O-H bonds
1100-1000	γ(C-C) skeletal vibrations from PVA chains
700	δ(O-H) deformation vibrations from C-O-H bonds

Broad band noted at 3600-3100 cm^{-1} was described as stretching vibrations of O-H bonds of PVA molecules present in UnMHs, obtained by crosslinking of PVA with borax at different ratios (3:1, 2:1 and 1:1 w/w). Within hydroxyl groups observed at 3600-3100 cm^{-1} range, borax anions were identified [34]. The absorption bands at 2930 and 2850 cm^{-1} were related to the asymmetrical and symmetrical stretching vibrations of the C-H bonds of CH_2 groups, present in the linear structure of PVA [35] and obtained UnMHs. The peak at 1740 cm^{-1} is characteristic for acetic groups derived from partial hydrolysis of polyvinyl acetate to polyvinyl alcohol [36]. At the wave number of approx. 1500-1300 cm^{-1}, deformation bands of C-H bonds of CH_2 groups located in the chains of PVA and obtained unmodified hydrogels can be observed [36]. Bands at 1250 and 1100 cm^{-1} were related to C-O stretching bonds from acetic groups and hydroxyl groups in PVA [36] and they slightly disappear in case of UnMHs. Peaks occurring at 1290 and 1130 cm^{-1} are characteristic for stretching vibrations of Borax-O-C groups and they confirm the formation of covalent bonds between PVA chains and Borax anions [36]. The intensity of mentioned bands increases with the growing amount of Borax in hydrogel compositions. To provide sufficient FTIR spectra analysis of CLHs (**Figure 6**) it was needed to perform detailed analysis of FTIR spectra of Cipro. Detailed band assignments were given in **Table 5**.

371 **Table 5.** Detailed band assignment of Fourier transform-infrared spectroscopy (FTIR) spectra
372 presented in Fig. 6 (CLHs and Cipro).
373

Wavelength [cm^{-1}]	Assignment
3500-3368	ν(O-H) stretching vibrations from hydroxyl groups, intramolecular H-bonded
3035-3011	ν(C-H) and ν(Ar-H) from aromatic cyclic enes
2927, 2907	ν(C-H) asymmetrical and symmetric stretching vibrations from CH_2 groups
2697-2457	ν(>C=O) and ν (>N-<|) stretching vibrations from COOH and N-bonded and NH
1702	ν(C=O) stretching vibrations from carbonyl
1625-1603	Quinolines, δ(N-H) bending vibrations
1556	δ(C-H) deformation vibrations from CH_2 groups
1494-1386	ν(C-O) stretching vibrations from carbonyl groups
1333-1211	δ(O-H) bending vibrations of hydroxyl groups
1050-1033	ν(C-F) stretching vibrations of C-F bond, fluorine group

374

375 **Table 6.** Detailed band assignment of Fourier transform-infrared spectroscopy (FTIR) spectra
376 presented in Fig. 6(CLHs, H4-H5).
377

Wavelength [cm^{-1}]	Assignment
3615-3001	ν(O-H) stretching vibrations from hydroxyl groups of PVA and H1, H2, H3 hydrogels
2923	ν(C-H) symmetrical stretching vibrations from CH_2 groups
2848	ν(C-H) asymmetrical stretching vibrations from CH_2 groups
1727	ν(C=O) stretching vibrations from acetyl groups
1674-1627	Quinolines, δ(N-H) bending vibrations
1333	ν(B-O-C) stretching vibrations from H1, H2 and H3 hydrogels
1274	ν(C-O) stretching vibrations from acetyl groups
1180	ν(B-O-C) stretching vibrations from H1, H2 and H3 hydrogels
1106	ν(C-O) stretching vibrations from C-O-H bonds
1025-950	γ(C-C) skeletal vibrations from PVA chains
823, 770	δ(O-H) deformation vibrations from C-O-H bonds

378

379 The prominent and characteristic peak for Cipro was identified between 3500-3368 cm^{-1}. It was
380 assigned to an O-H stretching vibration (intermolecular hydrogen bonding). Band observed
381 between 3035-3011 cm^{-1} represented alkenes and aromatic C-H stretching, related to stretching
382 vibrations of aromatic enes. Bands at 2927 cm^{-1} and 2907 cm^{-1} were described as asymmetric
383 and symmetric stretching vibrations coming from CH_2 groups. In the range of 2697-2457 cm^{-1}
384 stretching vibrations of C=O and >N- coming from COOH and N-bonded were identified. Band
385 at 1702 cm^{-1} showed carbonyl stretching vibrations in the Cipro molecule. Range of 1625-1603
386 cm-1 shows N-H bending vibrations of Quinolines. At 1556 cm^{-1} deformation vibrations of C-
387 H from CH_2 groups were observed. Range of 1494-1386 cm^{-1} represented C-O stretching
388 vibrations from carbonyl and carboxylic acid groups. In between 1333 and 1211 cm^{-1} bending
389 vibrations of hydroxyl groups were observed. Finally, the range between 1050-1033 cm^{-1}

Analysis of CLHs FTIR spectra (**Fig. 6**) did not reveal large differences in band assignments (**Table 6**), with one significant exception. Bands observed in the range between 1674-1627 cm^{-1} were not noted in case of UnMHs, but were identified in case of Cipro FTIR spectra analysis (**Table 5**). This bands were assigned to Quinolines, δ(N-H) bending vibrations, what could confirm presence of Cipro in CLHs.

3.2.2. Scanning electron microscopy (SEM) with Energy-dispersive X-ray spectroscopy (EDX)

CLHs surface (**Table 2**, H4-H6) were studied by SEM imaging (**Fig. 7**). H4 hydrogel was characterized by a surface at which craterous-like pattern was observed. Single crater-like structure sizes were in the range of 2-5 μm. Observed craterous-like structures were distributed evenly over the entire surface of H4 CLH. This structure seems to be interesting according to the potential place of Cipro bonding in a CLH and its further release from CRH network. Craterous-like structures were not identified further for H5 and H6 hydrogel.

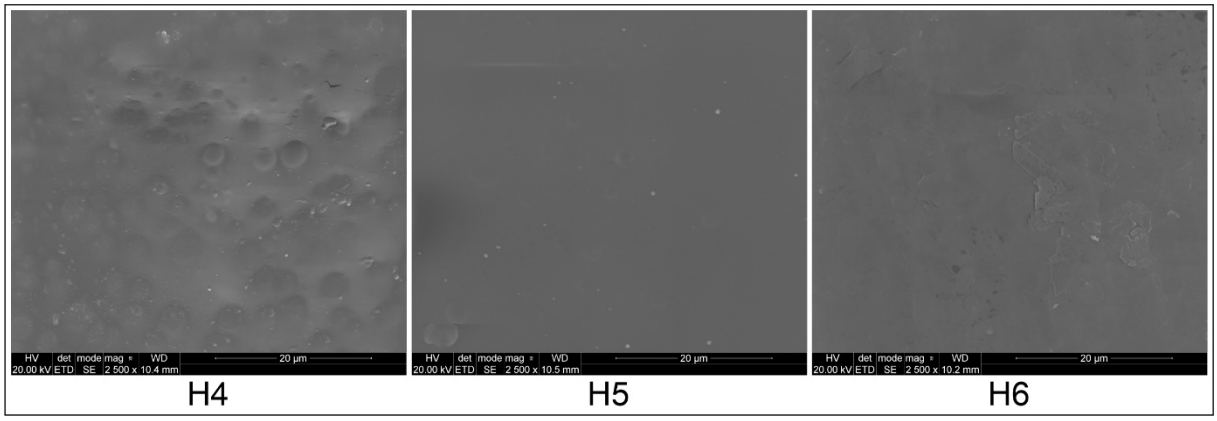

Figure 7. Selected SEM images showing craterous-like structures at the surface of H4 CLH and lack of these structures at the surface of H5 and H6 CLHs. Magnification 2500x.

EDX spectra (**Figure 8**) confirmed presence of such elements like carbon and oxygen, which were core of polymers used in CLHs fabrication. Fluorine and chlorine presence may be additional confirmation of Cipro presence in CLH. This would suggest successful hydrogels modification. Detected sodium element can come from unreacted Borax used as a hydrogels crosslinker. This would suggest that further purification process could be thought after CLHs synthesis. Samples were sputtered with gold before testing; therefore peaks from Au were present.

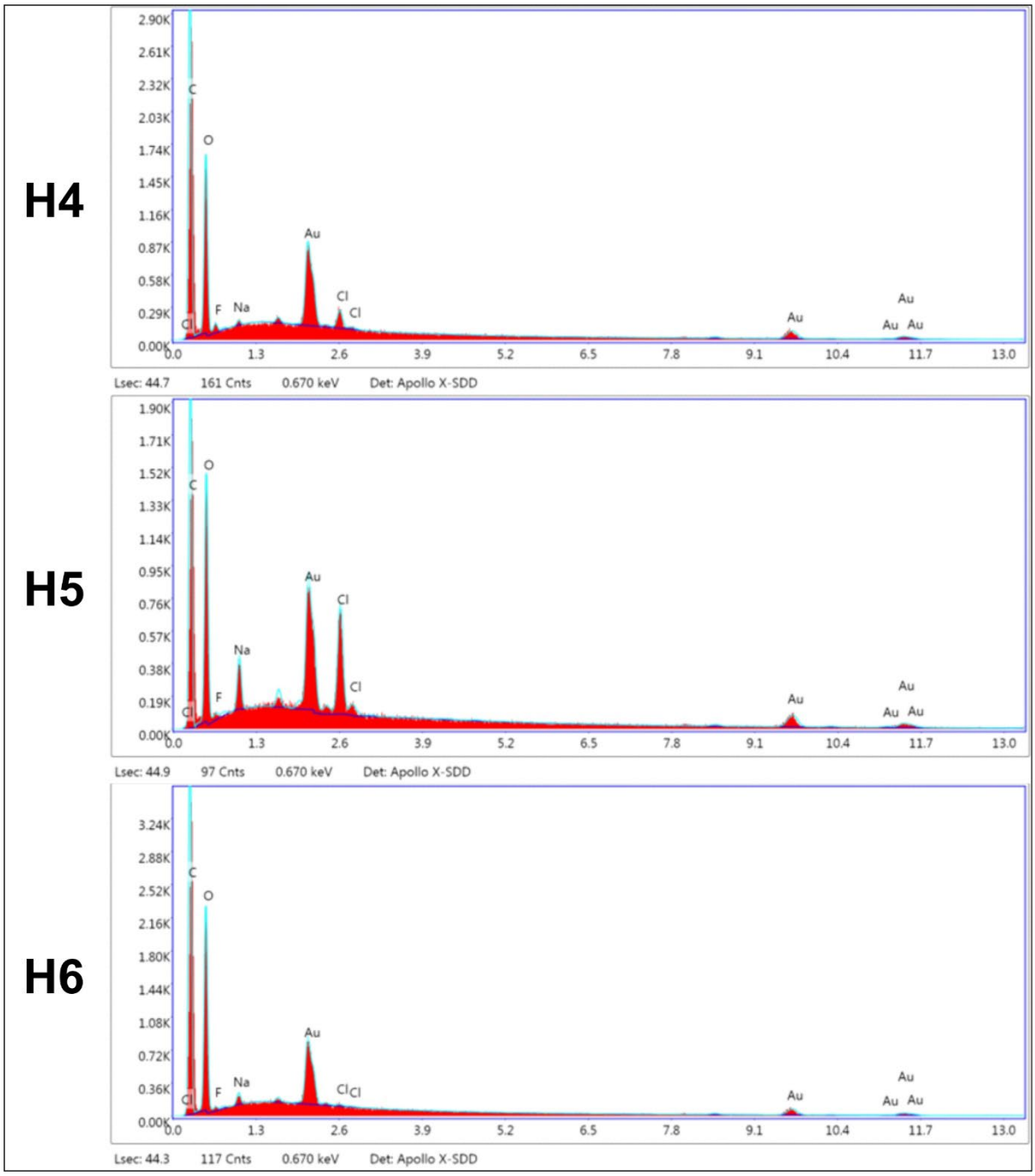

Figure 8. EDX spectra of H4-H6 of CLHs.

The results of EDX analysis (**Figure 8, Table 7**) of CLHs revealed that H6 sample was characterized by the slightly higher atomic content of fluorine (1.33 ± 0.05%). For H4 and H5 hydrogels atomic content of fluorine reached 0.44 ± 0.03% and 0.58 ± 0.03%, respectively. Based on this analysis, we can assume, that slightly higher Cipro content was enclosed in H6 hydrogel. One-way ANOVA and Tukey test evaluated that all those values were statistically different ($\alpha = 0.05$).

425 **Table 7.** Weight and atomic content of elements in H4, H5 and H6 hydrogels.

426

Element	H4		H5		H6	
	Weight %	Atomic %	Weight %	Atomic %	Weight %	Atomic %
C	53.95 ± 0.34	61.21 ± 0.34	53.92 ± 0,41	62.64 ± 0.50	56.87 ± 0.16	64.25 ± 0.19
O	44.24 ± 0.36	37.67 ± 0.33	38.22 ± 0.81	33.34 ± 0.69	39.83 ± 0.41	33.78 ± 0.33
F	0.61 ± 0.05	0.44 ± 0.03	0.79 ± 0.04	0.58 ± 0.03	1.86 ± 0.07	1.33 ± 0.05
Na	1.08 ± 0.01	0.64 ± 0.01	3.15 ± 0.07	1.91 ± 0.04	0.46 ± 0.13	0.27 ± 0.07
Cl	0.11 ± 0.07	0.04 ± 0.03	3.92 ± 0.31	1.54 ± 0.12	0.98 ± 0.06	0.38 ± 0.02

427

428

429 Growing trace of carbon in hydrogels was observed along with the growing PVA/borax ratio.
430 For example, one-way ANOVA evaluation and Tukey test confirmed that for H4 sample
431 (PVA/borax = 1:1 w/w) C atomic content was slightly lower (61.21 ± 0.34%) than for H6
432 sample (64.25 ± 0.19%) with PVA/borax ratio equal 3:1 w/w ($\alpha = 0.05$). In the case of oxygen
433 content, for H4, H5 and H6 values were close to be equal 37.67 ± 0.33%, 33.34 ± 0.69% and
434 33.78 ± 0.33%, respectively. One-way ANOVA and Tukey test evaluated that oxygen content
435 for H4 was significantly higher than for H5 and H6, which were statistically the same ($\alpha =$
436 0.05). Statistical analysis of H4, H5 and H6 samples confirmed the impact of the PVA/borax
437 ratio on the carbon, oxygen and fluorine content in the tested hydrogels.

438 3.3. Hybrid Cipro-Loaded Wound Dressings (H-CLWDs) Characterization

439 3.3.1. Short-term degradation (STD) study

440 **Figure 9** and **Figure 10** showed mass loss of obtained H-CLWDs, calculated after short-term
441 degradation assessment in acidic (2M HCl) and alkali (5M NaOH) media respectively. Each
442 type of biomaterial may be considered as possibly degradable in physiological conditions. It
443 was observed that in the alkali environment all of the tested samples were characterized by the
444 higher average mass loss than in the acidic medium. In the alkali environment degradation rates
445 were approximately 13% and 19% higher than in the acidic conditions after 7^{th} and 14^{th} day
446 respectively ($\alpha = 0.05$). For instance, after 14^{th} day of degradation PUR/10PVA showed 49.58
447 ± 4.29% and 69.08 ± 4.47% mass loss in HCl and NaOH respectively. Moreover, two-way
448 ANOVA examination revealed that, in both acidic and basic environment, the type of composite
449 based on PLA or PVA had a strong impact on the mass loss results ($\alpha = 0.05$). Obtained results
450 and two-way ANOVA test revealed, that for H-CLWD obtained by using PVA (PUR/10PVA,
451 PUR/20PVA and PUR/30PVA), the mass loss was significantly higher than for H-CLWDs
452 made by using PUR combined with PLA: PUR/10PLA, PUR/20PLA and PUR/30PLA ($\alpha =$

0.05) for both acidic and alkali media. For example, after 14th day of assessment in HCl, for PUR/20PLA mass loss reached 26.01 ± 4.78% and for PUR/20PVA it was equal to 50.89 ± 6.03%. **Figure 11** shows mass loss of obtained H-CLWDs degradation assessment in solution mimicking physiological fluids (0.01M PBS). The study confirms findings from degradation in acid and alkali media. The highest degradation after 56 days was observed for PUR/30PVA (24.55 ± 1.88%) and the lowest for PUR/10PLA (12.00 ± 0.57%). Two-way ANOVA examination revealed that both the type of composite (PLA or PVA) and the concentration of additive (PLA or PVA) concentration had a strong impact on the mass loss results on 14th day and 56th day ($\alpha = 0.05$). On 28th day the impact of composite type was not statistically important.

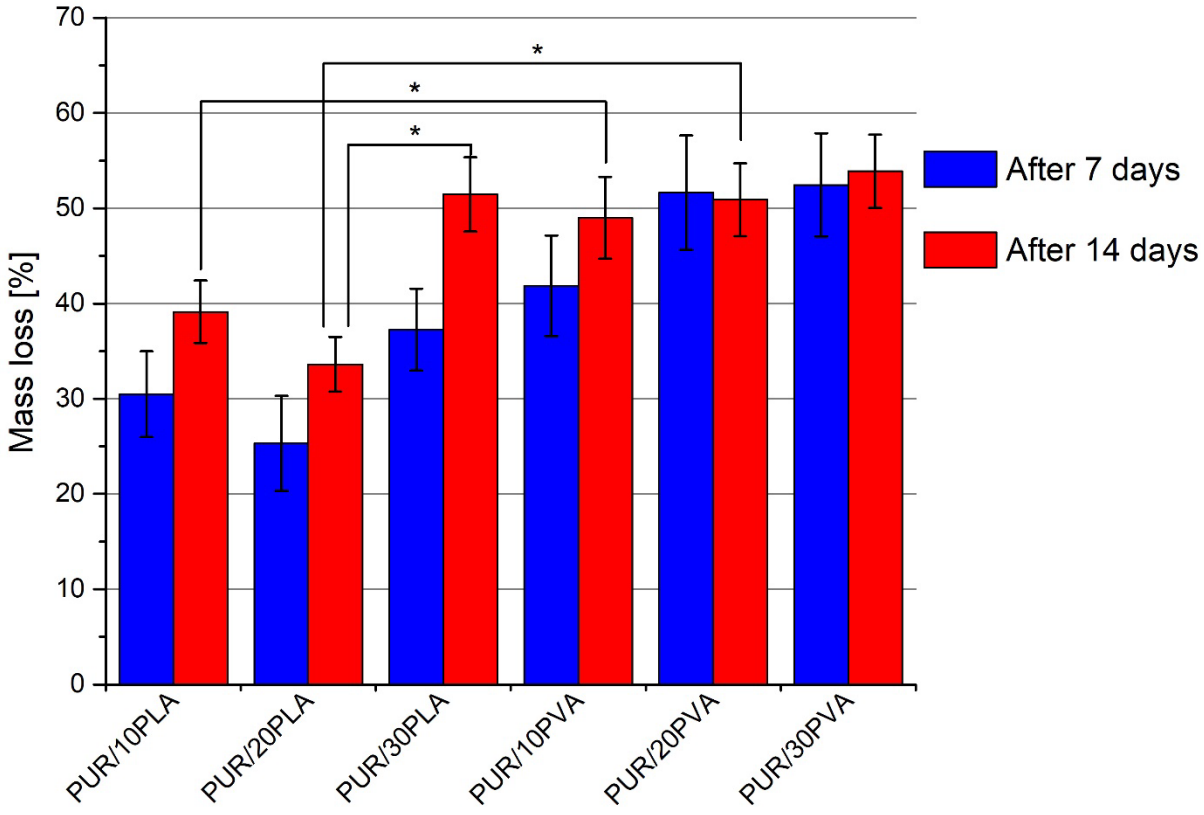

Figure 9. Average mass loss of H-CLWDs based on PUR and PLA composition in 2M HCl (* samples significantly different: $\alpha = 0.05$, n=3).

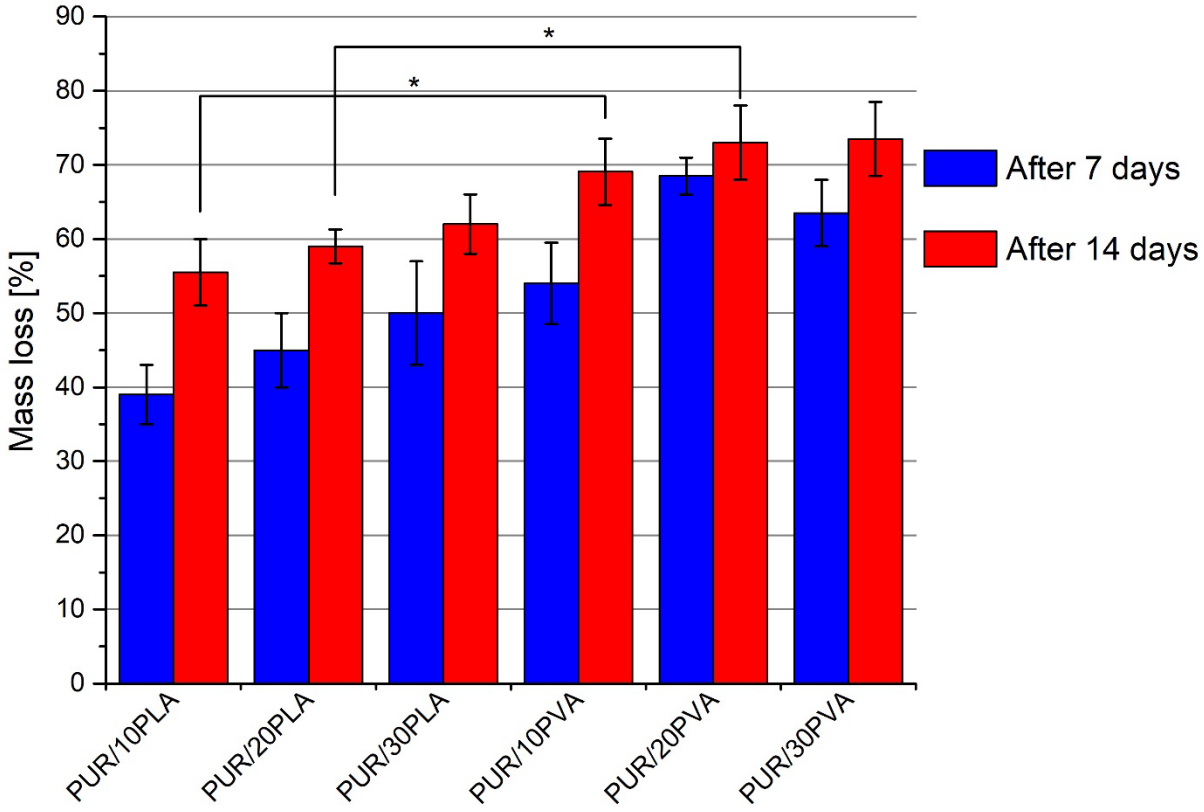

Figure 10. Average mass loss of H-CLWDs based on PUR/PLA or PUR/PVA composition in 5M NaOH (* samples significantly different: $\alpha = 0.05$, n=3).

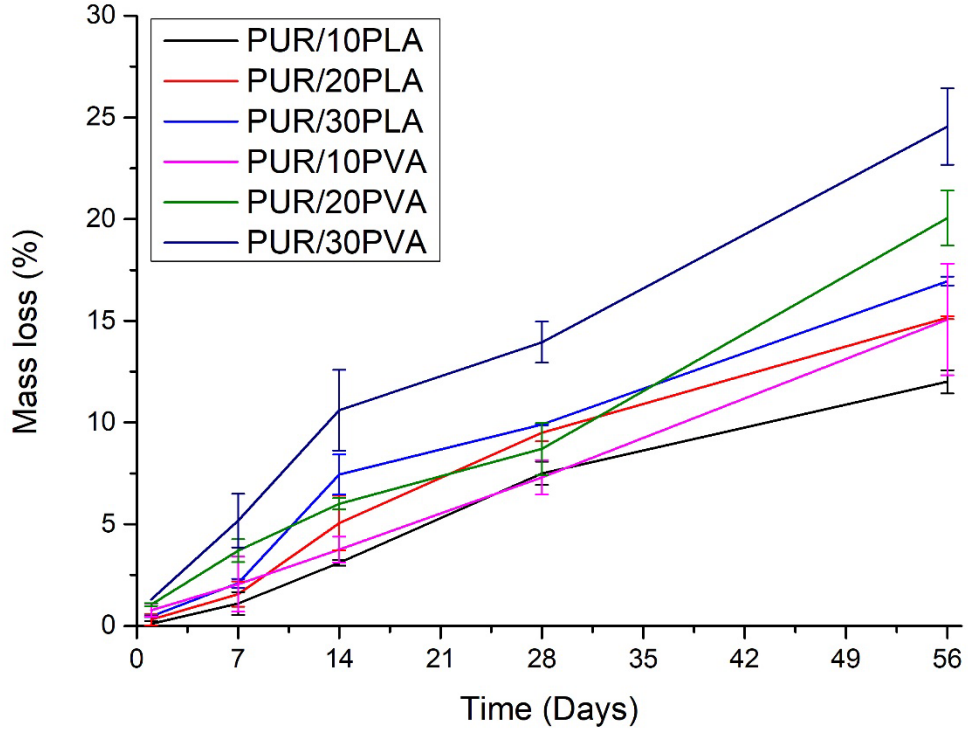

Figure 11. Average mass loss of H-CLWDs based on PUR/PLA or PUR/PVA composition in 0.01M PBS.

3.3.2. High Performance Liquid Chromatography

HPLC (**Fig. 12**) was used to determine the release of ciprofloxacin hydrochloride from obtained composite dressings after short-term (5 and 15 minutes **- Figures 13-14**) and long-term (1 and 7 days – **Figures 15-16**) exposure to hydrolytic conditions. **Figure 13** showed the amount of released Cipro, depending on the type of hydrogel and matrix used to obtain composite dressing. These values were also converted into Cipro content per 1 μg of the dressing (**Figure 14**). It was observed that all the produced dressings show the ability to release Cipro. According to **Figure 13**, D6 was characterized by the highest Cipro release for both 5 and 15 minutes (18.7 ± 1.8 μg/ml and 21.76 ± 0.64 μg/ml, respectively) in comparison to the rest of tested materials. It was also evaluated that for dressings PUR/30PVA: (D4, D5, D6) the concentrations of eluted drugs were approximately 9% and 3% higher on average (for 5 and 15 min, respectively) than for D1, D2, D3 matrices ($\alpha = 0.05$). Obtained results may be related to higher porosity of D4, D5, D6 PUR/30PVA matrices. Additionally, it was observed that the type of used hydrogel also had strong impact on Cipro releasing process. For example, after 15 min of releasing for D1, D2 and D3 patches (**Figure 13**) containing PUR/30PLA porous matrices, the quantity of Cipro increased with the growing proportion of PVA and borax solutions (from 13.0 ± 2.2 μg/ml for D1 to 18.1 ± 1.3 μg/ml for D3). The same situation can be observed for D4, D5 and D6 patches including PUR/30PVA matrices. For D4 with PVA/borax solutions ratio equal to 1:1 w/w, amount of released Cipro after 15 min ranged 17.2 ± 1.5 μg/ml and for D6 with PVA/borax solutions ratio it was equal 21.76 ± 0.64 μg/ml. **Figures 15-16** showed results of prolongated release studies for D6 composite dressing. Performed one-way ANOVA test proved that released drug values were not statistically different after 15 min of test ($\alpha = 0.05$).

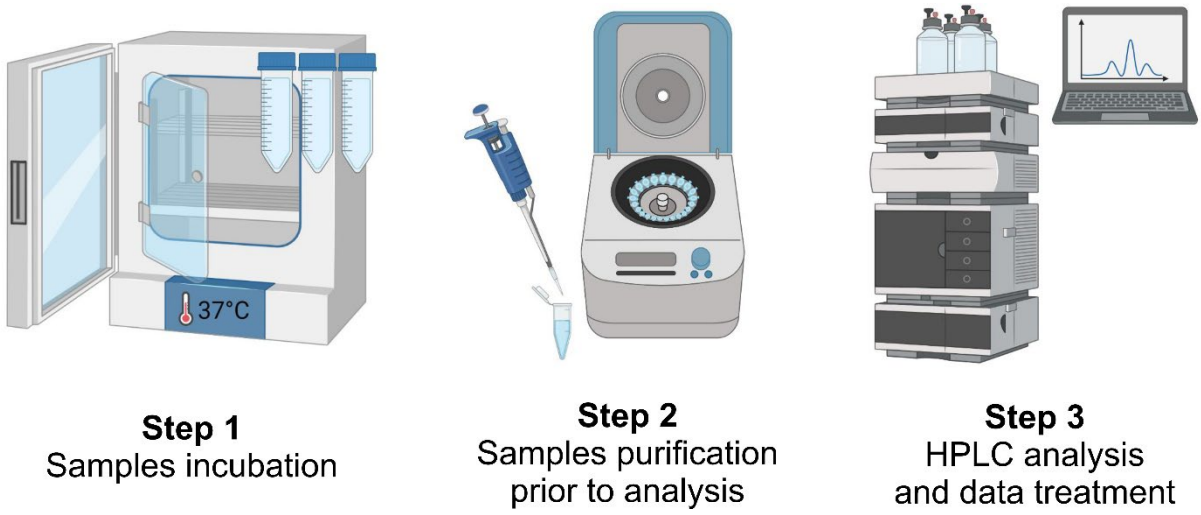

497

498 **Figure 12.** Scheme of sample preparation for determination of Cipro released in time.

499

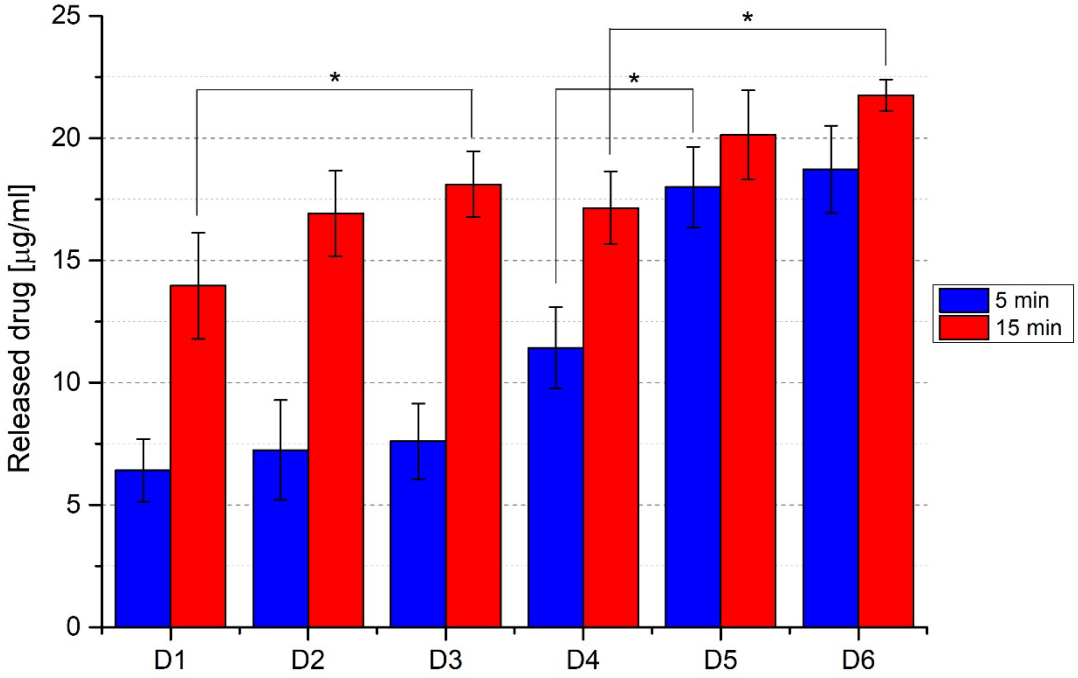

500

501 **Figure 13.** Concentration of released Cipro after 5 and 15 min for D1, D2, D3, D4, D5 and

502 D6 composite dressings (* samples significantly different: $\alpha = 0.05$, n=3).

503

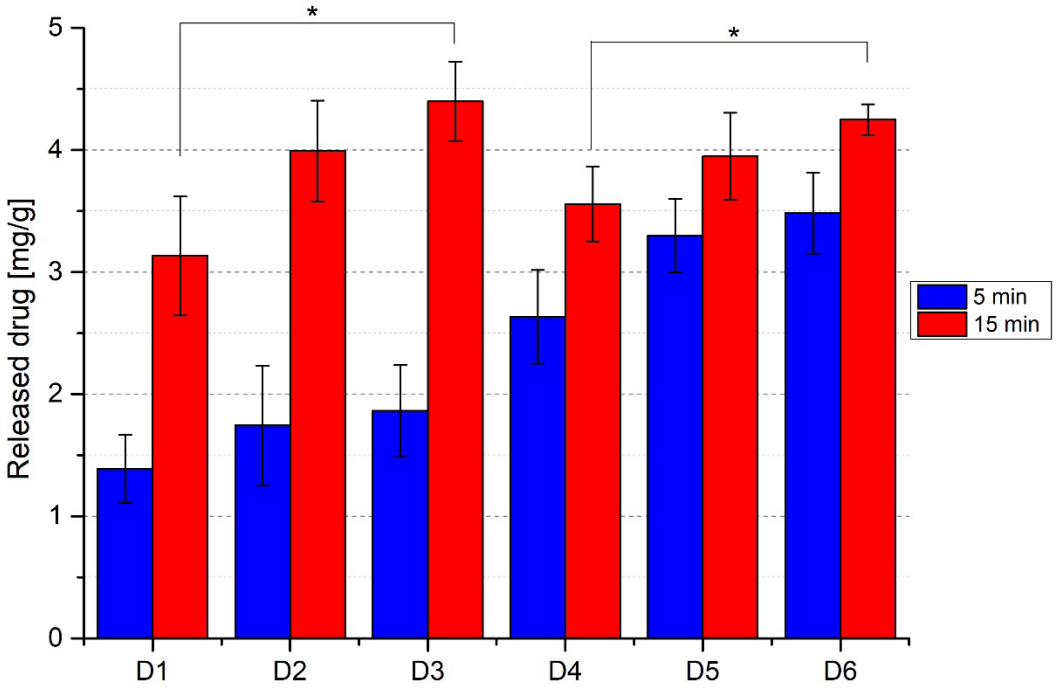

504

505 **Figure 14.** Amount of released Cipro after 5 and 15 min for D1, D2, D3, D4, D5 and D6

506 composite dressings per 1 mg of dressing (* samples significantly different: $\alpha = 0.05$, n=3).

507

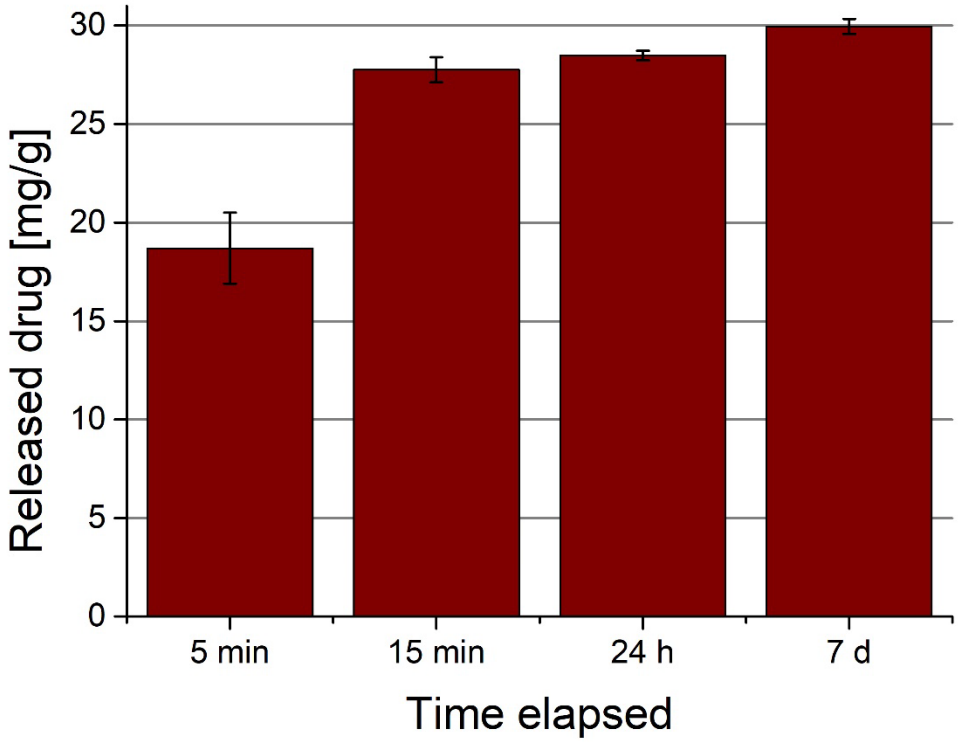

508

509 **Figure 15.** Amount of released Cipro after 5 and 15 min, 24 h and 7 d for D6 composite
510 dressing.

511

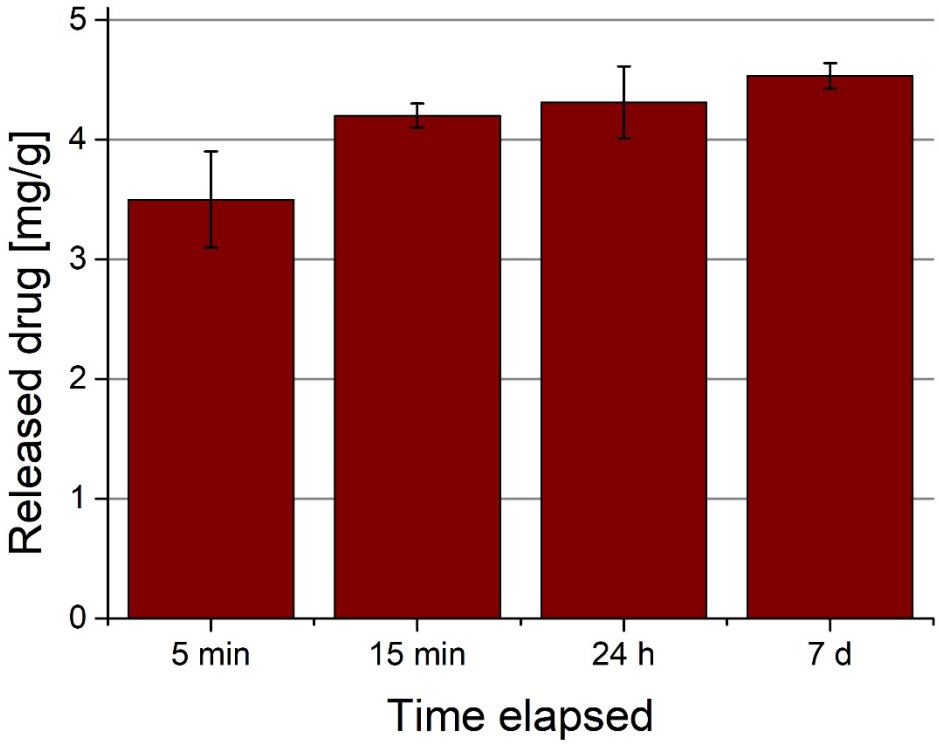

512

513 **Figure 16.** Amount of released Cipro after 5 and 15 min, 24 h and 7 d for D6 composite
514 dressing per 1 mg of dressing.

515

516 3.4. Biological performance of H-CRWDs

517 3.4.1. Microbiology tests

518 Performed microbiology tests showed that both types of obtained H-CRWDs based on PLA
519 and PVA showed significant bacterial growth inhibition zones (**Figure 17)**. This clearly
520 confirmed that Cipro introduced to such kind of hybrid dressing revealed antibacterial activity
521 against *S. aureus*.

522

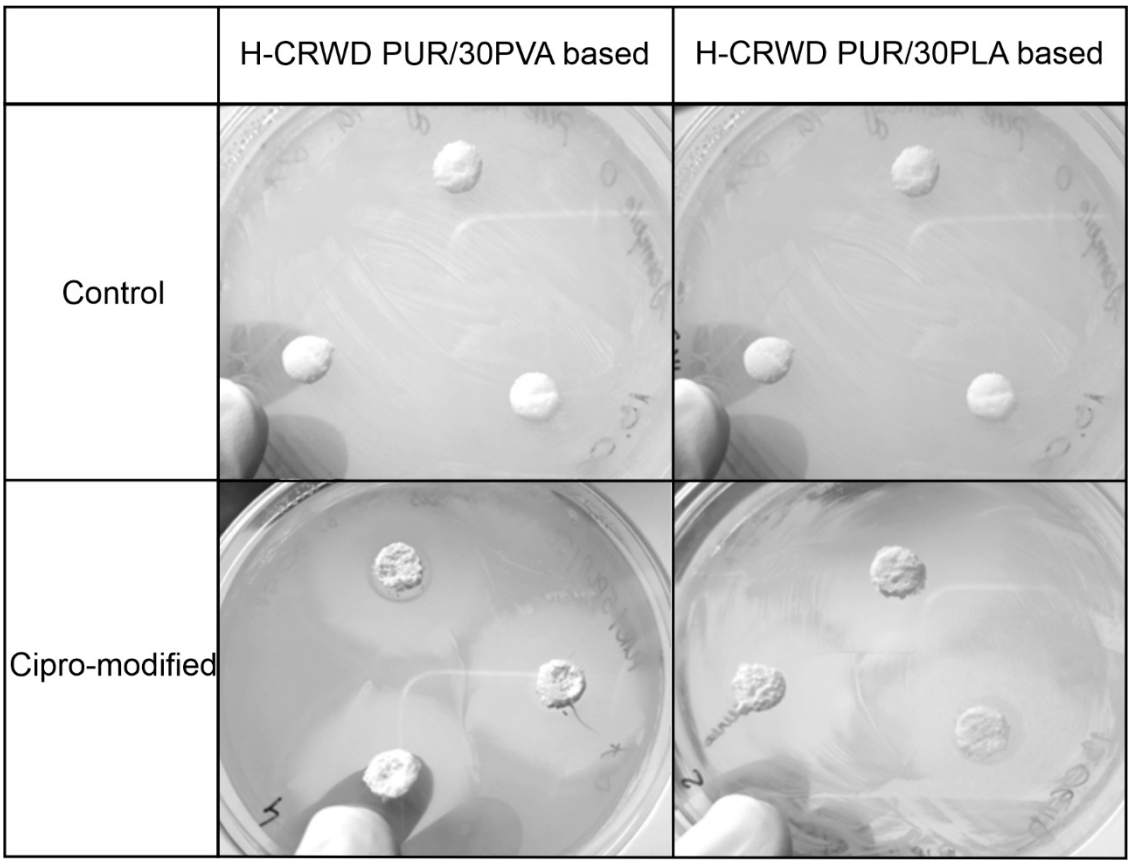

Figure 17. Inhibition zones of *S. aureus* growth observed for H-CRWD in comparison to Control (hybrid wound dressing not loaded with Cipro).

3.4.2. Cytotoxicity Assay

Analysis of **Figure 18** showed that obtained H-CRWDs with the use of PUR/30PVA were representing satisfactory biocompatibility levels at variety of extract concentrations. It could be seen that at 100% extract concentration the cell viability was lower in comparison to other concentrations (50%-12.5%). We assume few causes for this effect. First of them could be the fact, that obtained materials, despite fabrication methods using a lot of flushing, may need development of additional purification methods. Additionally, LAA used for CLHs modification may still be present in the H-CRWDs structure and impact cells growth. Despite this nuisance, obtained materials were considered as biocompatible according to ISO 109993-5 standard. Optical microscope images (**Figure 19**) confirmed this fact. Obtained H-CRWDs by using PUR/30PVA allowed morphology maintenance of CCl163 cell line. Presence of 1.5 wt% of Cipro in this systems was not disturbing neither cell growth nor their morphology.

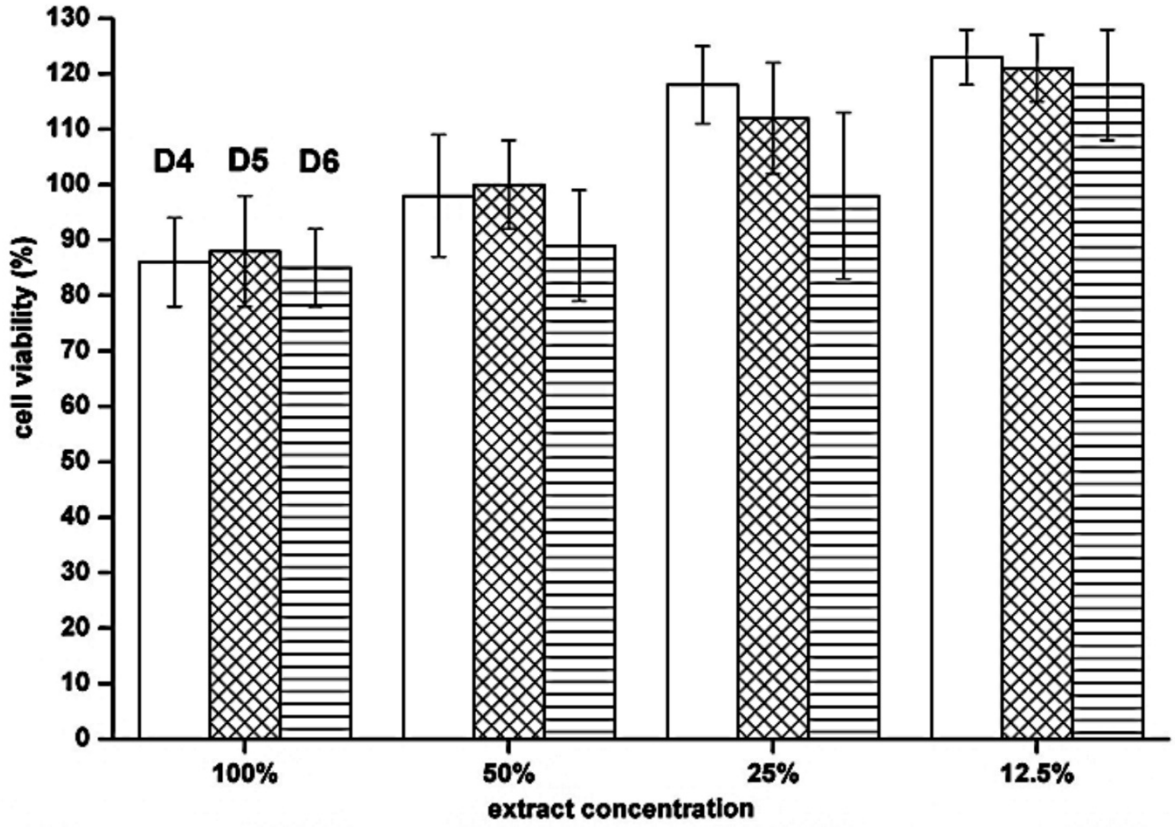

Figure 18. Cell viability of CCl163 cells depending on extract concentration.

Sample/ Extract Concentration	0%	100%	75%	50%	12.5%
D4					
D5					
D6					

Figure 19. Morphology of CCI163 cells after 24h contact with extracts at different concentrations.

4. Discussion

548 Skin is one of the most important organs of human body and development of its functional
549 substitutes are one of the highly demanded products, because chronic wounds treatment like
550 burns, ulcers or infected wounds belongs to one of the biggest challenges of XXIst century. In
551 the case of small, uninfected wounds no medical intervention is necessary due to the high ability
552 of the skin to regenerate. For chronic wounds and large burns the process of natural regeneration
553 is much more complicated, often impossible or lasts long. One of the modern solutions for
554 problems associated with healing of skin injuries is the application of different types of wound
555 dressings selected for specific types of wounds. In this paper we proposed as a promising
556 solution a H-CRWD composed of CPMs based on PUR/30PVA and CLHs releasing Cipro in
557 vitro.
558 The solid porous matrices of CPMs were based either on PUR/PLA composition either
559 PUR/PVA composition (10-30 wt%). Average porosity of CPMs was in the range of 69-81%
560 and the highest porosity values were observed for composites containing of 30 wt% either PUR
561 either PLA. On this basis CPMs consisting of PUR/30PLA or PUR/30PVA were selected for
562 further fabrication of H-CRWDs. What is worth to mention is the fact that CPMs composed of
563 PUR/PVA had of 5% higher porosity then those composed of PUR/PLA. Type of composition
564 had an effect on CPMs porosity. The higher porosity the better scaffold availability for cells to
565 diffuse through the scaffold [38] and controlled degradation [39,40] due to the equal medium
566 flow through the scaffold. Based on porosity CPMs obtained with the use of PUR/PVA
567 composition seemed to be more favorable for skin engineering at this stage of studies.
568 Pore sizes of CPMs obtained by using PUR/PLA were in the range from 123-68 μm and pore
569 sizes of PUR/10PLA were statistically higher than other two described compositions. In case
570 of PUR/PVA compositions pore sizes were in the range from 88-103μm and were not
571 statistically different for described compositions. In literature Chitrattha et al. [41] obtained
572 composite porous dressings consisted of PLA and PEG loaded with gentamicin sulphate (GS)
573 or metronidazole (MZ). Their porosities differed from 53 ± 2% to 55 ± 2% and they were
574 characterized by high antimicrobial activity against e.g. *S. aureus*. O'Brien et al. evaluated that
575 the suitable pore size for skin tissue regeneration was in the range of 20 – 120 μm. The pore
576 size of obtained CPMs was similar, thus optimal for cell migration, adhesion and proliferation
577 favouring with skin regeneration [42,43].
578 Obtained hydrogels were studied by FTIR spectroscopy. FTIR spectra analysis confirmed
579 presence of Cipro in obtained CLHs. Bands observed between 1674 and 1627 cm^{-1} were
580 assigned as bending vibration of N-H related to the quinolines, what found a confirmation in
581 other literature data [37]. Slight spectra shift was observed when ratio of PVA:Borax was

changed from 1:1 to 3:1 in obtained hydrogels, but it did not influence chemical structure enough to impact hydrogels behavior within further characterization studies.

SEM analysis of UnMHs showed craterous-like surface for H4 hydrogel, which was not noted for other types of UnMHs or CLHs. EDX results were another asset confirming presence of fluorine and chlorine in obtained CLHs. Due to lack of proof in literature, this surface defects can be treated as anomaly.

Short-term degradation studies determined that H-CRWDs were degrading faster in basic and acidic media if CPMs were obtained with the use of PUR/PVA composition in comparison to these CPMs obtained by using PUR/PLA composition. It could be caused by ease of hydrolysis process observed for PVA compared to PLA, due to the fact that PVA is a polymer soluble in water [44,45]. In this case, PVA occurred to act as a more favorable "fast-degradable polymer", what would be an asset in skin engineering expecting tissue scaffold to degrade within a suitable time frame. Those results were confirmed with degradation studies in physiological fluid-like medium (0.01 M PBS).

Studied drug release of H-CRWD based on PUR/30PVA composition revealed that the concentration of eluted Cipro was approximately 9% and 3% higher in average (after 5 and 15 min, respectively) than for H-CRWD based on PUR/30PLA composition. Prolongated studies on D6 sample showed that amount of released drug was not changed after 15 min of the test. It could be caused by difficulties of active substance transport from inner parts of the sample. It is worth noting that swelling is related to drug release, and swelling is mainly dependent from area of contact between hydrogel and medium [46]. The active substance release can be then lower in H-CRWD than it would be expected from hydrogel, mostly because presence of polymer pores, which lowers the contact area and swelling ability.

Microbiology testing was another experiment, which confirmed successful Cipro-release of H-CRWDs. Bacterial growth inhibition zones were observed for both types of CPMs, but in case of CPMs obtained with the use of PUR/PVA compositions the growth inhibition zones (Fig. 14) were better distinguished in comparison to CPMs obtained with the use of PUR/PLA composition. It was related to drug released studies, because it was found out that PUR/PVA were releasing more of Cipro. Literature also proves presence of inhibition zones for Cipro-modified hydrogels [33].

Performed MTT assay, according to ISO 10993-5 standard, proved that obtained H-CRWDs based on PUR/30PVA were biocompatible (over 85% of cells viability at 100% of extract concentration) and did not disturb CCl163 cell morphology. It was also shown that presence of Cipro in the systems was not disturbing neither cell growth nor their morphology. Literature

presents both the significant reduction in cells viability [47] and biocompatibility of Cipro-loaded hydrogels [48]. Probably the Cipro acts differently with different cell assays, but in presented study, the MTT assay was performed accordingly to ISO 10993-5 standard and suitable assay.

Summarizing all the results, obtained H-CRWDs presented suitable characteristics to be considered as potential skin wound dressings. The best results were obtained for H6 prototypes produced using 30 wt% of PVA (PUR/30PVA) and a hydrogel made of 4% PVA, 1.5% Cipro and 10% AA solution and mixed with a borax solution in ratio 3:1 (w/w) (H6).

5. Conclusions

In this scientific paper we proposed a promising solution of H-CRWDs composed of CPM based on PUR/PVA and PUR/PLA mixes and CLHs releasing Cipro *in vitro* (21.76 ± 0.64 µg/ml after 15 min). Simple and cost-effective methods were used to obtain H-CRWDs components; CMPs were obtained by SC/PL and CLH simply by mixing PVA with Borax at different ratios. Performed physicochemical studies, morphology analysis, drug-release studies, short term degradation studies and biological performance verification lead to the conclusion that only one system was favorable for application as skin wound dressing and it was H-CRWD based on PUR/30PVA composition and hydrogel made of 4% PVA, 1.5% Cipro and 10% AA and mixed with a borax solution in ratio 3:1 (w/w). This system showed the highest degradation (up to 53% mass loss in 2M HCl, 72% in 5M NaOH after 14 days and up to 25% mass loss in 0.01M PBS after 56 days), and highest Cipro *invitro* release (up to 4 mg of Cipro per 1 g of wound dressing after 15 minutes). Cipro-loaded system showed significant inhibition zones against *S. aureus*. Presented wound dressing prototypes showed also biocompatibility accordingly to ISO 10993-5 standard (over 85% cell viability at 100% extract). With the use of this material we will continue to design and develop new solutions to provide easy to do and affordable solutions to treat chronic wounds of high potential to become infected wounds, thus antibacterial effect is in great demand.

Data Availability

The raw/processed data required to reproduce these findings cannot be shared at this time as the data also forms part of an ongoing study.

References

649
650 [1] Granick MS, Sood A, Tomaselli NL. Wound Dressings and Comparative Effectiveness
651 Data 2014;3:511–29. https://doi.org/10.1089/wound.2012.0401.
652 [2] Nosrati H, Aramideh Khouy R, Nosrati A, Khodaei M, Banitalebi-Dehkordi M, Ashrafi-
653 Dehkordi K, et al. Nanocomposite scaffolds for accelerating chronic wound healing by
654 enhancing angiogenesis. J Nanobiotechnology 2021;19:1–22.
655 https://doi.org/10.1186/s12951-020-00755-7.
656 [3] Sadeghzade S, Emadi R, Labbaf S. Hardystonite-diopside nanocomposite scaffolds for
657 bone tissue engineering applications. Mater Chem Phys 2017;202:95–103.
658 https://doi.org/10.1016/j.matchemphys.2017.09.018.
659 [4] Liu H, Wang C, Li C. RSC Advances dressing and drug delivery system in the treatment
660 of wound healing. RSC Adv 2018;8:7533–49. https://doi.org/10.1039/C7RA13510F.
661 [5] Kopecki Z. Development of next-generation antimicrobial hydrogel dressing to combat
662 burn wound infection. Biosci Rep 2021. https://doi.org/10.1042/BSR20203404.
663 [6] Saghazadeh S, Rinoldi C, Schot M, Saheb S, Shari F, Jalilian E, et al. Drug delivery
664 systems and materials for wound healing applications ☆ 2018;127:138–66.
665 https://doi.org/10.1016/j.addr.2018.04.008.
666 [7] Thaarup IC, Bjarnsholt T. Current in vitro biofilm-infected chronic wound models for
667 developing new treatment possibilities. Adv Wound Care 2021;10:91–102.
668 https://doi.org/10.1089/wound.2020.1176.
669 [8] Xu Z, Han S, Gu Z, Wu J. Advances and Impact of Antioxidant Hydrogel in Chronic
670 Wound Healing. Adv Healthc Mater 2020;9:1901502.
671 https://doi.org/10.1002/adhm.201901502.
672 [9] Borda LJ, Macquhae FE, Kirsner RS. Wound Dressings : A Comprehensive Review.
673 Curr Dermatol Rep 2016. https://doi.org/10.1007/s13671-016-0162-5.
674 [10] Vilar G, Tulla-puche J, Albericio F. Polymers and Drug Delivery Systems 2018:1–28.
675 [11] Zhang X, Shu W, Yu Q, Qu W, Wang Y, Li R. Functional Biomaterials for Treatment
676 of Chronic Wound. Front Bioeng Biotechnol 2020;8:516.
677 https://doi.org/10.3389/fbioe.2020.00516.
678 [12] Koehler J, Brandl FP, Goepferich AM. Hydrogel Wound Dressings for Bioactive
679 Treatment of Acute and Chronic. Eur Polym J 2017.
680 https://doi.org/10.1016/j.eurpolymj.2017.12.046.
681 [13] Unnithan AR, Barakat NAM, Pichiah PBT, Gnanasekaran G, Nirmala R, Cha Y, et al.
682 Wound-dressing materials with antibacterial activity from electrospun polyurethane –

dextran nanofiber mats containing ciprofloxacin HCl. Carbohydr Polym 2012;90:1786–93. https://doi.org/10.1016/j.carbpol.2012.07.071.

[14] Vermeulen H, Ubbink DT, Goossens A, Vos R De, Legemate DA. Systematic review of dressings and topical agents for surgical wounds healing by secondary intention 2005:665–72. https://doi.org/10.1002/bjs.5055.

[15] Miraftab M, Collyer G. A critical review of modern and emerging absorbent dressings used to treat exuding wounds 2012:1–12. https://doi.org/10.1111/j.1742-481X.2011.00923.x.

[16] Chattopadhyay S, Raines RT. Review Collagen-Based Biomaterials for Wound Healing 2014;101. https://doi.org/10.1002/bip.22486.

[17] Yao C, Lee C, Huang C, Chen K. Novel bilayer wound dressing based on electrospun gelatin/keratin nanofibrous mats for skin wound repair. Mater Sci Eng C 2017. https://doi.org/10.1016/j.msec.2017.05.076.

[18] Alarcon EI, Baker AB. Biomaterials and Nanotherapeutics for enhancing Skin wound Healing 2016;4:1–20. https://doi.org/10.3389/fbioe.2016.00082.

[19] Pott FS, Meier MJ, Ribas JD. La efectividad del hidrocoloide versus otros apósitos en la cicatrización de úlceras por presión en adultos y ancianos : revisión sistemática y metanálisis 1 Introducción Método 2014;22:511–20. https://doi.org/10.1590/0104-1169.3480.2445.

[20] K PS, Babu M. Collagen based dressings Ð a review 2000;26:54–62.

[21] Queen D, Orsted H, Sanada H, Sussman G. A dressing history 2004;1.

[22] Ono S, Imai R, Ida Y, Shibata D, Komiya T, Matsumura H. ScienceDirect Increased wound pH as an indicator of local wound infection in second degree burns. Burns 2014;41:820–4. https://doi.org/10.1016/j.burns.2014.10.023.

[23] Boateng JS, Matthews KH, Stevens HNE, Eccleston GM. Wound Healing Dressings and Drug Delivery Systems : A Review. J Pharm Sci 2008;97:2892–923. https://doi.org/10.1002/jps.21210.

[24] Leaper DJ, Schultz G, Carville K, Fletcher J, Swanson T, Drake R. Extending the TIME concept : what have we learned in the past 10 years ?* 2012.

[25] Gogolewski S, Gorna K, Zaczynska E, Czarny A. Structure-property relations and cytotoxicity of isosorbide-based biodegradable polyurethane scaffolds for tissue repair and regeneration. J Biomed Mater Res - Part A 2008;85:456–65. https://doi.org/10.1002/jbm.a.31481.

[26] Grzesiak J, Marycz K, Szarek D, Bednarz P, Laska J. Polyurethane/polylactide-based

biomaterials combined with rat olfactory bulb-derived glial cells and adipose-derived mesenchymal stromal cells for neural regenerative medicine applications. Mater Sci Eng C 2015;52:163–70. https://doi.org/10.1016/j.msec.2015.03.050.

[27] Gubanska I, Kucinska-Lipka J, Janik H. The influence of amorphous macrodiol, diisocyanate type and L-ascorbic acid modifier on chemical structure, morphology and degradation behavior of polyurethanes for tissue scaffolds fabrication. Polym Degrad Stab 2019;163:52–67. https://doi.org/10.1016/j.polymdegradstab.2019.02.025.

[28] Chen H, Xing X, Tan H, Jia Y, Zhou T, Chen Y, et al. Covalently antibacterial alginate-chitosan hydrogel dressing integrated gelatin microspheres containing tetracycline hydrochloride for wound healing. Mater Sci Eng C 2017;70:287–95. https://doi.org/10.1016/j.msec.2016.08.086.

[29] Bergman B, Bishop MC, Bjerklund-johansen TE, Botto H, Lobel B, Cruz FJ, et al. EAU Guidelines for the Management of Urinary and Male Genital Tract 2001:576–88.

[30] Sripriya R, Kumar MS. Journal of Biomaterials Science , Collagen bilayer dressing with ciprofloxacin , an effective system for infected wound healing 2012:37–41. https://doi.org/10.1163/156856207779996913.

[31] Choipang C, Chuysinuan P, Suwantong O, Ekabutr P, Supaphol P. AC. J Drug Deliv Sci Technol 2018. https://doi.org/10.1016/j.jddst.2018.06.025.

[32] Kucińska-Lipka J. Polyurethanes crosslinked with poly(vinyl alcohol) as a slowly-degradable and hydrophilic materials of potential use in regenerative medicine. Materials (Basel) 2018;11. https://doi.org/10.3390/ma11030352.

[33] Iga C, Agata T, Marcin Ł, Natalia F, Justyna KL. Ciprofloxacin-modified degradable hybrid polyurethane-polylactide porous scaffolds developed for potential use as an antibacterial scaffold for regeneration of skin. Polymers (Basel) 2020;12:171. https://doi.org/10.3390/polym12010171.

[34] Devi S.A., Philip D. AG. Infrared, Polarized Raman, and SERS Spectra of Borax. J Solid State Chem 1994;113:157–62.

[35] Brady J., Dürig T., Lee P.I. LJX. Chapter 7 - Polymer Properties and Characterization, Developing Solid Oral Dosage Forms (Second Edition), Pharmaceutical Theory and Practice. 2017.

[36] Marin E, Rojas J, Ciro Y. A review of polyvinyl alcohol derivatives: Promising materials for pharmaceutical and biomedical applications. African J Pharm Pharmacol 2014;8:674–84. https://doi.org/10.5897/AJPP2013.3906.

[37] Sahoo S, Chakraborti C, Mishra S. Qualitative analysis of controlled release

ciprofloxacin/carbopol 934 mucoadhesive suspension. J Adv Pharm Technol Res 2011;2:195. https://doi.org/10.4103/2231-4040.85541.

[38] Kucińska-Lipka J, Gubanska I, Skwarska A. Microporous polyurethane thin layer as a promising scaffold for tissue engineering. Polymers (Basel) 2017;9:1–16. https://doi.org/10.1023/B:WATE.0000026525.82039.ef.

[39] Ballarin FM, Caracciolo PC, Blotta E, Ballarin VL, Abraham GA. Optimization of poly (L -lactic acid)/ segmented polyurethane electrospinning process for the production of bilayered small-diameter nano fi brous tubular structures. Mater Sci Eng C 2014;42:489–99. https://doi.org/10.1016/j.msec.2014.05.074.

[40] Montini-Ballarin F, Caracciolo PC, Rivero G, Abraham GA. In vitro degradation of electrospun poly(l-lactic acid)/segmented poly(ester urethane) blends. Polym Degrad Stab 2016;126:159–69. https://doi.org/10.1016/j.polymdegradstab.2016.02.007.

[41] Chitrattha S, Phaechamud T. Porous poly (DL -lactic acid) matrix fi lm with antimicrobial activities for wound dressing application. Mater Sci Eng C 2016;58:1122–30. https://doi.org/10.1016/j.msec.2015.09.083.

[42] Brien FJO, Harley BA, Yannas I V, Gibson LJ. The effect of pore size on cell adhesion in collagen-GAG scaffolds 2005;26:433–41. https://doi.org/10.1016/j.biomaterials.2004.02.052.

[43] Pietramaggiori G, Erba P. Foam Pore Size Is a Critical Interface Parameter n.d.:589–97. https://doi.org/10.1097/PRS.0b013e3182402c89.

[44] Pal K, Banthia AK, Majumdar DK. Polyvinyl alcohol-gelatin patches of salicylic acid: Preparation, characterization and drug release studies. J Biomater Appl 2006;21:75–91. https://doi.org/10.1177/0885328206056312.

[45] Goyanes A, Kobayashi M, Martínez-Pacheco R, Gaisford S, Basit AW. Fused-filament 3D printing of drug products: Microstructure analysis and drug release characteristics of PVA-based caplets. Int J Pharm 2016;514:290–5. https://doi.org/10.1016/j.ijpharm.2016.06.021.

[46] Bouklas N, Huang R. Swelling kinetics of polymer gels: comparison of linear and nonlinear theories. Soft Matter 2012;8:8194. https://doi.org/10.1039/c2sm25467k.

[47] Du J, El-Sherbiny IM, Smyth HD. Swellable Ciprofloxacin-Loaded Nano-in-Micro Hydrogel Particles for Local Lung Drug Delivery. AAPS PharmSciTech 2014;15:1535–44. https://doi.org/10.1208/s12249-014-0176-x.

[48] Bruk LA, Dunkelberger KE, Khampang P, Hong W, Sadagopan S, Alper CM, et al. Controlled release of ciprofloxacin and ceftriaxone from a single ototopical

785 administration of antibiotic-loaded polymer microspheres and thermoresponsive gel.
786 PLoS One 2020;15:e0240535. https://doi.org/10.1371/journal.pone.0240535.
787